

Title

Stroma-derived Insulin-like growth factors enhance chemoresistance in pancreatic cancer.

Running title

Stroma-derived IGFs enhance chemoresistance in PDA

Key words

Macrophages, myofibroblasts, Insulin-like growth factors, chemoresistance, pancreatic cancer.

Authors

Lucy Ireland ^{1#}, Almudena Santos ^{1#}, Muhammad S. Ahmed ¹, Carolyn Rainer ¹, Sebastian R. Nielsen ¹, Valeria Quaranta ¹, Ulrike Weyer-Czernilofsky ², Danielle D. Engle ^{3,4}, Pedro Perez-Mancera ¹, Sarah E. Coupland ¹, Azzam Taktak ⁵, Thomas Bogenrieder ^{6,7}, David A. Tuveson ^{3,4,8}, Fiona Campbell ¹, Michael C. Schmid ¹ & Ainhoa Mielgo ^{1*}

These authors contributed equally to this work.

Affiliations

¹ Department of Molecular and Clinical Cancer Medicine. University of Liverpool. Liverpool L69 3GE, UK.

² Boehringer Ingelheim RCV GmbH & Co KG

Pharmacology and Translational Research, Vienna A-1121, Austria.

³ Cold Spring Harbor Laboratory, Cold Spring Harbor, NY 11724, USA.

⁴ Lustgarten Pancreatic Cancer Research Laboratory, Cold Spring Harbor, NY 11724, USA.

⁵ Department of Medical Physics and Clinical Engineering

Royal Liverpool University Hospital, Liverpool L7 8XP, UK.

⁶ Boehringer Ingelheim RCV GmbH & Co KG Medicine and Translational Research, Vienna, Austria.

⁷ Department of Urology, University Hospital Grosshadern, Ludwig-Maximilians-University, Marchioninistrasse 15, 81377 Munich, Germany

⁸ Rubenstein Center for Pancreatic Cancer Research, Memorial Sloan Kettering Cancer Center, New York, NY 10065, USA.

Correspondence

* author to whom correspondence should be addressed:

Dr Ainhoa Mielgo

Department of Molecular & Clinical Cancer Medicine, Institute of Translational Medicine

First Floor Sherrington Building, Ashton street, Liverpool L69 3GE

Phone: +44 (0) 151 794 9555

e-mail: amielgo@liverpool.ac.uk

Disclosures

The authors disclose no potential conflicts of interest.

Abstract

Pancreatic ductal adenocarcinoma (PDA) is one of the deadliest cancers and more effective therapies are urgently needed. Resistance to therapy is one of the biggest challenges in cancer treatment, including PDA. One dominant player in drug resistance is the presence of a rich pro-tumoral microenvironment. Tumor associated macrophages (TAMs) and myofibroblasts are key drivers of this pro-tumoral microenvironment, and have been associated with drug resistance in many cancers. However, our understanding of the molecular mechanisms by which TAMs and fibroblasts contribute to chemoresistance is still emerging. In these studies, we found that TAMs and myofibroblasts directly support chemoresistance of pancreatic cancer cells by secreting Insulin-like growth factors 1 and 2 (IGFs), which activate Insulin/IGF receptors on pancreatic cancer cells. Immunohistochemical analysis of biopsies from pancreatic cancer patients revealed that

72% of the patients express activated Insulin/IGF receptors on the tumor cells, and this positively correlates with increased CD163+ TAMs infiltration. Importantly, *in vivo*, we found that TAMs and myofibroblasts are the main sources of IGF production, and pharmacological blockade of IGFs sensitized pancreatic tumors to gemcitabine. These findings suggest that inhibition of IGFs in combination with chemotherapy could benefit pancreatic cancer patients, and that Insulin/IGF1R activation may be used to identify pancreatic cancer patients who could benefit from a combination of chemotherapy with anti-IGF signaling inhibitors.

Introduction

Drug resistance is one of the biggest challenges in cancer therapeutics and the cause of relapse in the majority of cancer patients [1, 2]. Therefore, understanding the molecular mechanisms by which cancer cells become resistant to therapies is critical to the development of durable treatment strategies. Mechanisms of resistance to therapies can be tumor cell intrinsic or mediated by the tumor microenvironment [3]. We previously described intrinsic mechanisms of cancer cells resistance to targeted therapy and radiotherapy [4-6]. However, multiple factors can contribute to resistance to therapy and tumor progression, and one dominant player in solid cancers, and specifically in pancreatic cancer, is the presence of a rich pro-tumoral microenvironment [7-10]. In the pancreatic tumor microenvironment, macrophages and fibroblasts are the most abundant stromal cells, and engage in bidirectional interactions with cancer cells. Although tumor associated macrophages (TAMs) have the potential to kill cancer cells, we and others have shown that TAMs can promote tumor initiation, progression, metastasis, and also protect tumors from cytotoxic agents [11-23]. Indeed, TAMs can be polarized into M1-like inflammatory macrophages that will activate an immune response against the tumor, or into M2-like immunosuppressive macrophages that promote tumor immunity and tumor progression [7, 24-26]. Thus, therapeutics that can reprogram TAMs into M1-like macrophages or that specifically inhibit the pro-tumoral

functions of M2-like macrophages, rather than macrophage ablation therapies, may be more effective in the goal of restraining cancer progression [27, 28]. However, the understanding of the precise molecular mechanisms by which TAMs and CAFs support tumor progression, and the use of combination therapies simultaneously targeting both pro-tumoral stromal cells and cancer cells is only beginning to emerge.

Pancreatic ductal adenocarcinoma (PDA) is a devastating disease, with one of the worst survival rates, and current standard therapies are unfortunately not very effective [29, 30]. A characteristic feature of PDA is an excessive tumor microenvironment with infiltrated immune cells that include macrophages (TAMs), and high numbers of activated fibroblasts, also known as myofibroblasts [31-33]. In these studies, we sought to gain a better understanding of the mechanism(s) by which TAMs and myofibroblasts support resistance of pancreatic cancer cells to chemotherapy with the aim to find innovative treatment combinations using conventional cytotoxic agents with therapies targeting the pro-tumorigenic functions of stromal cells.

Materials and Methods

Generation of primary KPC-derived pancreatic cancer cells

The murine pancreatic cancer cells KPC FC1242 were generated in the Tuveson lab (Cold Spring Harbor Laboratory, New York, USA) isolated from PDA tumor tissues obtained from LSL-Kras^{G12D}; LSL-Trp53^{R172H}; Pdx1-Cre mice of a pure C57BL/6 background as described previously with minor modifications [34]. KPC cells were isolated in our laboratory from PDA tumor tissues obtained from LSL-Kras^{G12D}; LSL-Trp53^{R172H}; Pdx1-Cre mice in the mixed 129/SvJae/C57Bl/6 background as described previously [35] (for more details, see Supplementary Data).

Cell lines

SUIT-2 and MIA-PaCa-2 human pancreatic cancer cell lines were cultured in DMEM supplemented with 10% FBS, 1% penicillin/streptomycin, at 37°C, 5% CO₂ incubator. SUIT-2 cells were obtained in 2012 and MIA-PaCa-2 cells in 2010, and both were last authenticated by Eurofins in June 2016, and periodically tested and resulted negative for mycoplasma contamination.

Generation of primary macrophages, primary pancreatic myofibroblasts, macrophage (MCM) and myofibroblasts (MyoCM) conditioned media

Primary murine macrophages were generated by flushing the bone marrow from the femur and tibia of C57BL/6 or mixed 129/SvJae/C57Bl/6 (PC) mice followed by incubation for 5 days in DMEM containing 10% FBS and 10 ng/mL murine M-CSF (PeproTech). Primary human macrophages were generated by purifying CD14⁺ monocytes from blood samples obtained from healthy subjects using magnetic bead affinity chromatography according to manufacturer's directions (Miltenyi Biotec) followed by incubation for 5 days in DMEM containing 10% FBS and 50 ng/mL recombinant human M-CSF (PeproTech). Primary pancreatic stellate cells were isolated from C57BL/6 mice pancreas by density gradient centrifugation, and were activated into myofibroblasts by culturing them on uncoated plastic dishes in IMDM with 10% FBS.

To generate macrophage and myofibroblasts conditioned media, cells were cultured in serum free media for 24-36 h, supernatant was harvested, filtered with 0.45µm filter, concentrated using StrataClean Resin (Agilent Technologies) and immunoblotted for IGF1 and IGF2 (Abcam), or stored at -20°C.

Treatment with chemotherapy, macrophage conditioned media, blocking antibodies and recombinant IGF

SUIT-2, MIA-PaCa-2 and KPC-derived cells were cultured in DMEM with 2% FBS for 24 hours, pretreated for 3 hours with MCM, or MyoCM, recombinant IGF (Peprotech 100-11) at 100ng/ml, or IGF blocking antibody (abcam 9572) at 10 µg/ml followed by Gemcitabine (Sigma G2463) at 200nM, nab-paclitaxel 10, 100 or 1000nM, paclitaxel (Sigma T7402) at 200nM or 5-FU (Sigma F6627) at 100µM. Cells were harvested after 24 to 36 hours and analyzed for Annexin-V/PI staining by flow cytometry.

RTK arrays & immunoblotting

Cells were serum starved or treated with macrophage conditioned media for 30 min or 3h, harvested and lysed in RIPA buffer (150 mM NaCl, 10 mM Tris-HCl pH 7.2, 0.1% SDS, 1% Triton X-100, 5 mM EDTA) supplemented with a complete protease inhibitor mixture (SIGMA), a phosphatase inhibitor cocktail (Invitrogen), 1 mM PMSF and 0.2 mM Na₃VO₄. Cell lysates were analyzed with the Phospho-RTK Array Kit (R&D Systems). Immunoblotting analyses were performed using antibodies listed in Supplementary Data.

Syngeneic Orthotopic pancreatic cancer models

Two orthotopic syngeneic pancreatic cancer models and two IGF blocking antibodies were used in these studies. In one model, 1 X 10⁶ primary KPC^{luc/zsGreen} (zsGreen) cells (FC1242^{luc/zsGreen}) isolated from a pure C57Bl/6 background were implanted into the pancreas of immune-competent syngeneic C57Bl/6 six- to eight-week-old female mice, and tumors were established for one week before beginning treatment . Mice were administered i.p with Gemcitabine (100 mg/kg), IGF blocking antibody BI 836845 (100 mg/Kg) [36] kindly provided by Boehringer Ingelheim, or IgG isotype control antibody, every 2 -3 days for 10-15 days before harvest. The second model is described in Supplementary Data.

Gene expression

Total RNA was isolated from purified cells as described for Qiagen Rneasy protocol. Total RNA from entire pancreatic tumor tissues was extracted using a high salt lysis buffer

(Guadidine thiocynate 5 M, sodium citrate 2.5 uM, lauryl sarcosine 0.5% in H₂O) to improve RNA quality followed by purification using Qiagen Rneasy protocol. cDNA was prepared from 1µg RNA/sample, and qPCR was performed using gene specific QuantiTect Primer Assay primers from Qiagen. Relative expression levels were normalized to *gapdh* expression according to the formula $2^{-\Delta C_t}$ (Ct *gene of interest* – Ct *gapdh*) [37].

Analysis and quantification of immune cells in pancreatic tumors by flow cytometry

Single cell suspensions from murine pancreatic tumors were prepared by mechanical and enzymatic disruption in Hanks Balanced Salt Solution (HBSS) with 1 mg/mL Collagenase P (Roche) (for more details, see Supplementary Data).

Immunohistochemical analysis

Deparaffinization and antigen retrieval was performed using an automated DAKO PT-link. Paraffin-embedded human and mouse PDA tumors were immunostained using the DAKO envision+ system-HRP. Tissue sections were incubated for 1 hour at room temperature with primary antibodies described in Supplementary Data.

Immunofluorescence

Human and mouse PDA frozen tissue sections were fixed with cold acetone, permeabilized in 0.1% Triton, blocked in 8% goat serum and incubated overnight at 4°C with anti-phospho Insulin/IGFR (R&D), CD68 (DAKO, clone KP1), CK19 (abcam), CK11 (Cell signaling), αSMA (abcam) and EpCAM (BD Pharmingen).

Results

Macrophage derived IGFs activate Insulin and IGF1 receptors signaling in pancreatic cancer cells and induce chemoresistance

We and others have previously shown that inhibition of myeloid cell infiltration into tumors restrains cancer progression and increases response to chemotherapy [12, 14, 15, 18-22].

To gain a better understanding of the molecular mechanisms by which macrophages modulate pancreatic cancer cells' response to chemotherapy, we cultured human and mouse pancreatic cancer cells with macrophage conditioned media (MCM) from primary human and mouse macrophages in the presence or absence of the standard chemotherapeutic agent gemcitabine. Primary human and mouse macrophages were generated using macrophage colony stimulating factor 1 (M-CSF1), which favors an M2-like phenotype [38], which was further confirmed by high expression of CD206 (M2 macrophage marker) and lack of IL-12 (M1 macrophage marker) (Fig. S1A, B). We found, that MCM can directly induce chemoresistance of human and mouse pancreatic cancer cells to gemcitabine (Fig. 1A). Mechanistically, a phospho-receptor tyrosine kinase array of pancreatic cancer cells cultured in the presence or absence of MCM revealed that MCM induces the phosphorylation and activation of three receptor tyrosine kinases (RTKs), Insulin receptor (number 1), AXL receptor (number 2) and Ephrin receptor (number 3) (Fig. 1B). Insulin/ IGF1 receptor signaling is known to be involved in drug resistance in various cancers [39]. However, a direct role for macrophages in chemoresistance of pancreatic cancer via macrophage-dependent activation of the Insulin and IGF1 receptors has so far never been described. Thus, in this report, we furthered focused on investigating the role of Insulin/IGF1 receptor activation by macrophages in pancreatic cancer chemoresistance. Activation of Insulin and IGF1 receptors by macrophages was further confirmed by immunoblotting analysis (Fig. 1C) and by detection of tyrosine phosphorylation on Insulin and IGF1 receptors immunoprecipitated from SUIT-2 human pancreatic cancer cells cultured in the presence or absence of MCM (Fig. 1D). Insulin and IGF1 receptors can bind three ligands: Insulin, IGF-1 and IGF-2 [40]. We found that primary human and mouse macrophages express mRNA levels of *Igf-1* and *Igf-2* but not *Insulin* (Fig. 1E, F and Fig. S1C, D). We also found IGF1 and IGF2 proteins in primary human and mouse MCM and macrophage lysates (Fig.1G). However, we could hardly detect any expression of IGFs nor Insulin in pancreatic cancer cells (Fig. S1E). Thus, these findings suggest that activation of Insulin and IGF1 receptors on pancreatic cancer cells is triggered through paracrine macrophage-derived

IGF1/IGF2 signaling. Interestingly, alternatively (IL-4) activated M2 macrophages expressed higher levels of IGFs compared to classically (IFN γ /LPS) activated M1 macrophages (Fig. S1C, D). Immunoblotting analysis of SUIT-2 human pancreatic cancer cells and KPC-derived murine pancreatic cancer cells stimulated with MCM revealed that MCM activates Insulin/IGF1R signaling to a similar degree as recombinant IGF (Fig. 1H). Importantly, blockade of IGF ligands with an IGF neutralizing antibody was able to prevent macrophage-dependent activation of Insulin/IGF1 receptors and the downstream effectors IRS1, IRS2 and AKT (Fig. 2A), and to inhibit macrophage-induced chemoresistance of human and mouse pancreatic cancer cells to gemcitabine (Fig. 2B, C, D). In addition, recombinant IGF was sufficient to mediate resistance of pancreatic cancer cells to chemotherapy, in a similar way to MCM (Fig. 2C, D, E, F). In the absence of chemotherapy, treatment of tumor cells with MCM, IGF blocking antibody or recombinant IGF alone did not alter the survival or proliferation of cancer cells (Fig. S2A and B). *In vitro* exposure of pancreatic cancer cells to MCM was also able to enhance resistance of cancer cells to paclitaxel and 5-Fluorouracil (5-FU) (Fig. S3A, B and C). These findings suggest an important role for macrophage-derived IGFs in activating the insulin/IGF1 receptor survival signaling pathway in pancreatic cancer cells, and in enhancing resistance to chemotherapy.

Insulin and IGF receptors are activated on tumor cells in biopsies from pancreatic cancer patients, and this positively correlates with increased TAMs

We next evaluated whether the Insulin/IGF1 receptor signaling is activated in biopsies from pancreatic cancer patients, and whether this correlates with increased macrophage infiltration. Immunofluorescent and immunohistochemical staining of phospho-Insulin and phospho-IGF1 receptors in biopsies from PDA patients revealed that Insulin/IGF1R signaling is activated in pancreatic cancer cells in 38 out of 53 (~72%) consented patients (Fig. 3A, B, C, Fig. S4A, B, Tables S1 and S2). Similarly, immunofluorescent and immunohistochemical staining of CD68 (pan myeloid/macrophage marker) and CD163 (macrophage marker, commonly used to identify M2-like macrophages in human tissues), in

the same frozen and paraffin embedded human PDA samples, showed that pancreatic tumors are infiltrated by CD68+ and CD163+ macrophages which surround the phospho-Insulin/IGF1R + ductal epithelial pancreatic cancer cells (Fig. 3D and Fig. S4C, D). Since we observed that M2-like macrophages express IGF ligands (Fig. 1E, F, G and Fig. S1C, D), we subsequently analyzed, by immunohistochemistry, serial sections from PDA patients for the co-presence of CD163 + (M2-like) macrophages and phospho-Insulin/IGF1R+ tumor cells. Importantly, we found that activation of Insulin/IGF1 receptors positively correlates with increased infiltration of CD163+ (M2-like) macrophages (Fig. 3E, F, and Tables S1 and S2). Immunofluorescent co-staining of TAMs and IGFs confirmed that, in PDA patient samples, TAMs express both IGF1 and IGF2 (Fig. 3G).

TAMs and myofibroblasts are the main sources of IGFs in the pancreatic tumor microenvironment.

To determine whether TAMs are the main source of IGFs within the pancreatic tumor microenvironment, we orthotopically implanted murine primary pancreatic cancer cells derived from the genetically engineered mouse model of pancreatic cancer (LSL-Kras^{G12D}; LSL-Trp53^{R172H}; Pdx1-Cre mice; KPC) into syngeneic immune-competent recipient mice. H&E, immunohistochemical, and immunofluorescent stainings with CD68, CD206 and α SMA, and flow cytometry analysis of these tumors, showed that these mice developed PDA, and that similar to human PDA, these tumors are infiltrated by immune cells, including macrophages (Fig. 4A, B and Fig S5A), and are rich in α SMA+ myofibroblasts (Fig. S5A and B) [32, 41-43]. Importantly, murine PDA orthotopic tumors also showed phosphorylation of Insulin/IGF1R on tumor cells (Fig. 4A). In addition, similar to the orthotopically implanted PDA tumors, spontaneous PDA tumors derived from the genetically engineered KPC model also showed activation of Insulin/IGF1R on tumor cells surrounded by CD206+ TAMs and α SMA positive myofibroblasts (Fig. S6).

To determine whether *in vivo*, pancreatic TAMs are the main source of IGFs, we isolated TAMs (F4/80+ cells) from established orthotopic PDA tumors and assessed the expression levels of *Igf-1* and *Igf-2*. In agreement with our previous findings (Fig. 1E, F, F and Fig. 3G), we found that intra-tumoral macrophages isolated from murine pancreatic tumors express higher levels of *Igf-1* and *Igf-2* compared to F4/80- cells (Fig. 4C).

To further investigate this, we used a second KPC-derived cell line (FC1242) stably labelled with zsGreen reporter gene. As previously described, KPC-derived zsGreen cells were orthotopically implanted into the pancreas of syngeneic recipient mice (Fig. 4D). Tumors were harvested at day 23, and tumor cells (CD45-/zsGreen+), non-immune stromal cells (CD45-/zsGreen-), M1-like macrophages (CD45+/F4/80+/CD206-) and M2-like macrophages (CD45+/F4/80+/CD206+) were sorted by flow cytometry (Fig. S7A) and analyzed for the expression of *Igf-1* and *Igf-2*. This model further confirmed that orthotopic pancreatic tumors are infiltrated by both CD206+ (M2-like) and CD206- (M1-like) TAMs (Fig. 4E) and revealed that both CD206+ (M2-like macrophages) and α SMA+ stromal cells, also known as myofibroblasts, are the main sources of IGFs in pancreatic tumors (Fig. 4F, Fig. S7B). The ability of pancreatic myofibroblasts to produce IGFs was further assessed ex-vivo in myofibroblasts and myofibroblasts conditioned media (MyoCM) (Fig. S8A, B, C), as well as their capacity to enhance resistance of tumor cells to chemotherapy (Fig. S8D). Similarly, Tape et al., recently found, using a proteomic approach, that *in vitro*, fibroblasts exposed to KPC-derived cells produce IGF, which promotes proliferation and survival of pancreatic cancer cells [44]. In agreement with these findings, we also found high levels of IGF1 and IGF2 proteins in areas that are rich in macrophages and myofibroblasts in biopsied from PDA patients (Fig. S9).

Blockade of IGFs improves response to gemcitabine in a pre-clinical tumor model of pancreatic cancer

Macrophages and myofibroblasts are the most abundant non-malignant stromal cells within the tumor microenvironment in PDA [33]. Since we found that TAMs and myofibroblasts express IGFs in the pancreatic tumor microenvironment and stromal-derived IGFs enhances resistance of pancreatic cancer cells to chemotherapy *in vitro*, we hypothesize that inhibition of IGFs could increase pancreatic cancer response to chemotherapy *in vivo*.

To test this hypothesis, we treated mice bearing established orthotopic pancreatic tumors with control IgG antibody, gemcitabine alone, IGF blocking antibody (BI 836845) alone or gemcitabine combined with BI 836845 (Fig. 5A). As previously shown [22, 32, 41, 43], and similar to what is observed in PDA patients, gemcitabine alone had little or no effect on tumor growth in this model (Fig. 5B). Treatment with BI 836845 IGF blocking antibody alone, only showed a modest effect on tumor growth. In contrast, combination of gemcitabine with BI 836845 significantly reduced tumor growth (Fig. 5B). Analysis of immune cell populations within the different treatment groups showed an increase in F4/80+ macrophages in gemcitabine and gemcitabine + BI 836845 treated tumors (Fig. 5C and Fig. S10), however the ratio of CD206- (M1-like) and CD206+ (M2-like) macrophages within tumors remained the same in all treatment groups (Fig. 5D). In addition, the percentage of inflammatory monocytes (Ly6C⁺Ly6G⁻CD11b⁺F4/80⁻), Neutrophils/Myeloid derived suppressor cells (Gr1⁺CD11b⁺F4/80⁻) and cytotoxic CD8+ T lymphocytes (CD3⁺CD8⁺; CTL) remained similar in all treatment groups (Fig. 5C). Immunohistochemical analysis of tumors, showed that phosphorylation of Insulin and IGF1 receptors was decreased in tumors treated with BI 836845 IGF blocking antibody (Fig. 5E and Fig. S11). Importantly, immunohistochemical staining of cleaved caspase-3 revealed significantly higher levels of cell death in tumors treated with the combination of gemcitabine and BI 836845, compared to control, gemcitabine alone or BI 836845 alone groups (Fig. 5E, F).

To confirm these results, we repeated a similar experiment using a second KPC-derived cell line, and a commercially available IGF blocking antibody from abcam (ab9572). This second *in vivo* experiment yielded very similar results, and showed a significant decrease in tumor

growth in mice treated with the combination of gemcitabine/ IGF blocking antibody (Fig. 6A, B), a decrease in Insulin and IGF1 receptors phosphorylation (Fig. 6C and Fig. S11), and a strong increase in cleaved caspase 3 levels in tumors co-treated with gemcitabine and IGF blocking antibody (Fig. 6C). Combination of 5-FU or paclitaxel with BI 836845 only produced a slight decrease in tumor growth in this model (Fig. S12A, B), despite an increase in tumor cell death (Fig. S12C, D).

Taken together, these findings indicate that functional blockade of IGFs significantly increases the response of pancreatic tumors to gemcitabine *in vivo*.

Discussion

The data presented herein describe that stromal-derived IGFs are a critical inducer of chemoresistance in pancreatic cancer, and provide pre-clinical data that support the rationale for using IGF blocking antibodies in combination with gemcitabine for the treatment of pancreatic cancer (Fig. 6D). In these studies, we report a direct role for TAMs and myofibroblasts in chemoresistance of pancreatic cancer cells, and a paracrine signaling loop in which stromal-derived IGFs activate the Insulin/IGF1R survival signaling pathway and blunt response of pancreatic cancer cells to chemotherapy. A recent study describes how fibroblasts exposed to pancreatic cancer cells secrete IGF, and this leads to pancreatic cancer cell survival and proliferation *in vitro* [44]. In agreement with these findings, in this study, we further confirm that production of IGF by stromal cells occurs in pancreatic tumors *in vivo* and that both macrophages and myofibroblasts, are the two major sources of IGFs within the pancreatic tumor microenvironment. In addition, we found that in humans, the Insulin/IGF1R signaling pathway is activated in 38/53 (~72%) of PDA patient samples, and this strongly positively correlates with an increase in CD163+ (M2-like) TAMs.

Based on these findings, we explored the therapeutic opportunities of combining gemcitabine with IGF inhibition in pre-clinical models of pancreatic cancer, and found that indeed, inhibition of IGFs signaling increases response of pancreatic tumors to gemcitabine.

While IGF receptor inhibitors failed in the clinics [41, 45-47], two IGF blocking antibodies, MEDI-573 and BI 836845, are being evaluated in phase 2 clinical trials for metastatic breast cancer (MEDI-573), and metastatic breast cancer and castration-resistant prostate cancer (BI 836845) (Clinical trials.gov Identifiers: NCT02204072, NCT01446159, NCT02123823). In contrast to IGF1 receptor inhibitors, which only inhibit signaling through IGF1 receptor, IGF ligands blocking antibodies inhibit proliferative (but not metabolic) signaling through both IGF1 and Insulin receptors. The studies described here provide the proof-of-principle for further evaluation of IGF-blocking antibodies in combination with gemcitabine for the treatment of pancreatic cancer patients.

Despite extensive efforts invested in the clinical development of therapies against PDA, current standard treatments only exert a modest effect, and targeting only the tumor cells has not resulted in a significant improvement in patient outcome [30, 31]. The rich stromal compartment present in PDA is not inert, and instead provides a variety of non-malignant stromal cells and extracellular matrix proteins, which support tumor initiation, progression and drug resistance [11, 20, 22, 23, 32, 35, 41, 42]. Thus, therapies that target both the neoplastic cells and the pro-tumorigenic functions of the stromal compartment will likely achieve a better therapeutic response.

TAMs can enhance or limit the efficacy of chemotherapy depending on the tumor model, the tumor stage and/or the chemotherapeutic agent used. For example, chemoresistance is increased when cytotoxic agents increase M2-like macrophage infiltration via CCL2 [48] or CSF1 [21]. Macrophages can also impair host responses to chemotherapy by expressing cathepsins that activate chemoprotective T cells [18, 19] or by inducing the upregulation of cytidine deaminase, an enzyme that metabolizes nucleoside analogs [20]. TAMs

demonstrate a high degree of plasticity, and can be polarized into M1-like anti-tumorigenic and M2-like pro-tumorigenic macrophages [49]. Previous studies targeting signaling pathways necessary for the recruitment of macrophages or specific chemotactic factors (CCL2/PI3K γ /CSF1) have provided proof of concept that macrophages represent an attractive target to reduce tumor progression [13, 14, 21, 22, 41, 50]. However, dependent on the microenvironmental cytokine milieu, macrophages are not only promoting tumor growth, but they can also critically orchestrate an anti-tumor immune response [9]. Thus, therapies that aim to specifically inhibit the pro-tumorigenic functions of macrophages, while sparing their tumoricidal activity, could act as an alternative, and perhaps, more efficient approach than therapies that completely block macrophage recruitment to the tumor [27, 28]. In this regard, our studies indicate that IGF blockade increases pancreatic tumors' response to gemcitabine without affecting immune cell infiltration, including macrophage infiltration, or without affecting macrophage polarization. Interestingly, a recent elegant study, also describes macrophage derived IGF as a key driver of resistance to CSF-1R inhibition in glioblastoma [51].

In conclusion, our studies suggest that in PDA, stroma-derived IGFs can blunt the response to chemotherapy via an IGF-Insulin/IGF1R paracrine signaling axis, and provide the rationale for further evaluating the combination of gemcitabine with IGF signaling blockade in pancreatic cancer treatment.

Grant Support

These studies were supported by a Sir Henry Dale research fellowship to Dr Ainhoa Mielgo, jointly funded by the Wellcome Trust and the Royal Society (grant number 102521/Z/13/Z), a New Investigator research grant from the Medical Research Council to Dr Michael Schmid (grant number MR/L000512/1) and North West Cancer Research funding to Dr Ainhoa Mielgo and Dr Michael Schmid.

Acknowledgments

We thank Professors R O'Connor, G Cohen, M Clague, S Urbe and D Palmer for discussions and sharing reagents and protocols. We thank A Linford for technical help with Immunohistochemistry and N Bird for collecting blood from healthy volunteers. We thank Boehringer Ingelheim for providing us with the IGF blocking antibody BI 836845. We also acknowledge the Liverpool Tissue Bank for providing tissue samples, and the Liverpool Centre for Cell Imaging (CCI), the flow cytometry/cell sorting facility and the biomedical science unit for provision of equipment and technical assistance. We thank the patients and their families, as well as the healthy blood donors who contributed with tissue samples and blood donations to these studies.

References

1. Holohan C, Van Schaeybroeck S, Longley DB, and Johnston PG. Cancer drug resistance: an evolving paradigm. *Nat Rev Cancer* 2013; 13: 714-726.
2. McMillin DW, Negri JM, and Mitsiades CS. The role of tumour-stromal interactions in modifying drug response: challenges and opportunities. *Nat Rev Drug Discov* 2013; 12: 217-228.
3. Klemm F and Joyce JA. Microenvironmental regulation of therapeutic response in cancer. *Trends Cell Biology* 2015; 25: 198-213.
4. Mielgo A, Seguin L, Huang M, Camargo MF, Anand S, Franovic A et al. A MEK-independent role for CRAF in mitosis and tumor progression. *Nature Medicine* 2011; 17: 1641-5.
5. Seguin L, Kato S, Franovic A, Camargo MF, Lesperance J, Elliott KC et al. An integrin β_3 -KRAS-RalB complex drives tumour stemness and resistance to EGFR inhibition. *Nature Cell Biology* 2014; 16: 457-68.
6. Advani SJ, Camargo MF, Seguin L, Mielgo A, Anand S, Hicks AM et al. Kinase-independent role for CRAF-driving tumour radioresistance via CHK2. *Nature Communications* 2015; 3: 8154.
7. Noy R, and Pollard JW. Tumor-associated macrophages: from mechanisms to therapy. *Immunity* 2014; 41: 49-61.
8. Mantovani A, and Allavena P. The interaction of anticancer therapies with tumor-associated macrophages. *J Exp Med* 2015; 212: 435-445.
9. De Palma M, and Lewis CE. Macrophage regulation of tumor responses to anticancer therapies. *Cancer Cell* 2013; 23: 277-286.
10. Junttila MR, and de Sauvage FJ. Influence of tumour micro-environment heterogeneity on therapeutic response. *Nature* 2013; 501: 346-354.
11. Liou GY, Doppler H, Necela B, Edenfield B, Zhang L, Dawson DW, et al. Mutant KRAS-induced expression of ICAM-1 in pancreatic acinar cells causes attraction of macrophages to expedite the formation of precancerous lesions. *Cancer Discov* 2015; 5: 52-63.

12. Lin EY, Nguyen AV, Russell RG, and Pollard JW. Colony-stimulating factor 1 promotes progression of mammary tumors to malignancy. *J Exp Med* 2001; 193: 727-740.
13. Qian BZ, Li J, Zhang H, Kitamura T, Zhang J, Campion LR et al. CCL2 recruits inflammatory monocytes to facilitate breast-tumour metastasis. *Nature* 2011; 475: 222-225.
14. Qian BZ, Zhang H, Li J, He T, Yeo EJ, Soong DY et al. FLT1 signaling in metastasis-associated macrophages activates an inflammatory signature that promotes breast cancer metastasis. *J Exp Med* 2015; 212: 1433-1448.
15. Schmid MC, Avraamides CJ, Dippold HC, Franco I, Foubert P, Ellies LG, et al. Receptor tyrosine kinases and TLR/IL1Rs unexpectedly activate myeloid cell PI3kgamma, a single convergent point promoting tumor inflammation and progression. *Cancer Cell* 2011; 19: 715-727.
16. Schmid MC, Avraamides CJ, Foubert P, Shaked Y, Kang SW, Kerbel RS et al. Combined blockade of integrin-alpha4beta1 plus cytokines SDF-1alpha or IL-1beta potently inhibits tumor inflammation and growth. *Cancer Res* 2011; 71: 6965-6975.
17. Schmid MC, Franco I, Kang SW, Hirsch E, Quilliam LA, and Varner JA. PI3-kinase gamma promotes Rap1a-mediated activation of myeloid cell integrin alpha4beta1, leading to tumor inflammation and growth. *PLoS One* 2013; 8: e60226.
18. Shree T, Olson OC, Elie BT, Kester JC, Garfall AL, Simpson K et al. Macrophages and cathepsin proteases blunt chemotherapeutic response in breast cancer. *Genes Dev* 2011; 25: 2465-2479.
19. Bruchard M, Mignot G, Derangere V, Chalmin F, Chevriaux A, Vegran F, et al. Chemotherapy-triggered cathepsin B release in myeloid-derived suppressor cells activates the Nlrp3 inflammasome and promotes tumor growth. *Nat Med* 2013; 19: 57-64.
20. Weizman N, Krelin Y, Shabtay-Orbach A, Amit M, Binenbaum Y, Wong RJ, et al. Macrophages mediate gemcitabine resistance of pancreatic adenocarcinoma by upregulating cytidine deaminase. *Oncogene* 2014; 33: 3812-3819.
21. DeNardo DG, Brennan DJ, Rexhepaj E, Ruffell B, Shiao SL, Madden SF et al. Leukocyte complexity predicts breast cancer survival and functionally regulates response to chemotherapy. *Cancer Discov* 2011; 1: 54-67.
22. Mitchem JB, Brennan DJ, Knolhoff BL, Belt BA, Zhu Y, Sanford DE et al. Targeting tumor-infiltrating macrophages decreases tumor-initiating cells, relieves immunosuppression, and improves chemotherapeutic responses. *Cancer Res* 2013; 73: 1128-1141.
23. Nielsen SR, Quaranta V, Linford A, Emeagi P, Rainer C, Santos A et al. Macrophage-secreted granulins supports pancreatic cancer metastasis by inducing liver fibrosis. *Nature Cell Biology* 2016; 18: 549-560.
24. Murray PJ, and Wynn TA. Protective and pathogenic functions of macrophage subsets. *Nat Rev Immunol* 2011; 11: 723-737.
25. Ruffell B, Affara NI, and Coussens LM. Differential macrophage programming in the tumor microenvironment. *Trends Immunol* 2012; 33: 119-126.
26. Sica A, and Mantovani A. Macrophage plasticity and polarization: in vivo veritas. *J Clin Invest* 2012; 122: 787-795.
27. Quail DF, and Joyce JA. Microenvironmental regulation of tumor progression and metastasis. *Nat Med* 2013; 19: 1423-1437.
28. Bronte V, and Murray PJ. Understanding local macrophage phenotypes in disease: modulating macrophage function to treat cancer. *Nat Med* 2015; 21: 117-119.
29. Conroy T, Desseigne F, Ychou M, Bouche O, Guimbaud R, Becouarn Y et al. FOLFIRINOX versus gemcitabine for metastatic pancreatic cancer. *N Engl J Med* 2011; 364: 1817-1825.
30. Von Hoff DD, Ramanathan RK, Borad MJ, Laheru DA, Smith LS, Wood TE et al. Gemcitabine plus nab-paclitaxel is an active regimen in patients with advanced pancreatic cancer: a phase I/II trial. *J Clin Oncol* 2011; 29: 4548-4554.

31. Shibuya KC, Goel VK, Xiong W, Sham JG, Pollack SM, Leahy AM et al. Pancreatic ductal adenocarcinoma contains an effector and regulatory immune cell infiltrate that is altered by multimodal neoadjuvant treatment. *PLoS One* 2014; 9: e96565.
32. Gunderson AJ, Kaneda MM, Tsujikawa T, Nguyen AV, Affara NI, Ruffell B et al. Bruton's Tyrosine Kinase (BTK)-dependent immune cell crosstalk drives pancreas cancer. *Cancer Discov* 2015; 6: 270-85.
33. Feig C, Gopinathan A, Neesse A, Chan DS, Cook N, and Tuveson DA. The pancreas cancer microenvironment. *Clin Cancer Res* 2012; 18: 4266-4276.
34. Hingorani SR, Wang L, Multani AS, Combs C, Deramaudt TB, Hruban RH et al. Trp53R172H and KrasG12D cooperate to promote chromosomal instability and widely metastatic pancreatic ductal adenocarcinoma in mice. *Cancer cell* 2005; 7: 469-483.
35. Olive KP, Jacobetz MA, Davidson CJ, Gopinathan A, McIntyre D, Honess D et al. Inhibition of Hedgehog signaling enhances delivery of chemotherapy in a mouse model of pancreatic cancer. *Science* 2009; 324: 1457-1461.
36. Friedbichler K, Hofmann MH, Kroeze M, Ostermann E, Lamche HR, Koessl C et al. Pharmacodynamic and antineoplastic activity of BI 836845, a fully human IGF ligand-neutralizing antibody, and mechanistic rationale for combination with rapamycin. *Mol Cancer Ther* 2014; 13: 399-409.
37. Schmittgen TD, and Livak KJ. Analyzing real-time PCR data by the comparative C(T) method. *Nat Protoc* 2008; 3: 1101-1108.
38. Lawrence T, and Natoli G. Transcriptional regulation of macrophage polarization: enabling diversity with identity. *Nat Rev Immunol* 2011; 11: 750-761.
39. Denduluri SK, Idowu O, Wang Z, Liao Z, Yan Z, Mohammed MK et al. Insulin-like growth factor (IGF) signaling in tumorigenesis and the development of cancer drug resistance. *Genes Dis* 2015; 2: 13-25.
40. Pollak M. The insulin and insulin-like growth factor receptor family in neoplasia: an update. *Nat Rev Cancer* 2012; 12: 159-169.
41. Zhu Y, Knolhoff BL, Meyer MA, Nywening TM, West BL, Luo J et al. CSF1/CSF1R blockade reprograms tumor-infiltrating macrophages and improves response to T-cell checkpoint immunotherapy in pancreatic cancer models. *Cancer Res* 2014; 74: 5057-5069.
42. Pylayeva-Gupta Y, Das S, Handler JS, Hajdu CH, Coffre M, Koralov S, and Bar-Sagi D. IL-35 producing B cells promote the development of pancreatic neoplasia. *Cancer Discov* 2015; 6: 247-55.
43. Torres MP, Rachagani S, Soucek JJ, Mallya K, Johansson SL, and Batra SK. Novel pancreatic cancer cell lines derived from genetically engineered mouse models of spontaneous pancreatic adenocarcinoma: applications in diagnosis and therapy. *PLoS One* 2013; 8: e80580.
44. Tape CJ, Ling S, Dimitriadi M, McMahan KM, Worboys JD, Leong HS, et al. Oncogenic KRAS regulates tumor cell signaling via stromal reciprocation. *Cell* 2016; 165: 910-920.
45. Guha M. Anticancer IGF1R classes take more knocks. *Nat Rev Drug Discov* 2013; 12: 250.
46. King H, Aleksic T, Haluska P, and Macaulay VM. Can we unlock the potential of IGF-1R inhibition in cancer therapy? *Cancer Treat Rev* 2014; 40: 1096-1105.
47. Gradishar WJ, Yardley DA, Layman R, Sparano JA, Chuang E, Northfelt et al. Clinical and Translational Results of a Phase II, Randomized Trial of an Anti-IGF-1R (Cixutumumab) in Women with Breast Cancer That Progressed on Endocrine Therapy. *Clin Cancer Res* 2016; 22: 301-309.
48. Nakasone ES, Askautrud HA, Kees T, Park JH, Plaks V, Ewald AJ et al. Imaging tumor-stroma interactions during chemotherapy reveals contributions of the microenvironment to resistance. *Cancer Cell* 2012; 21: 488-503.
49. Mills CD, Lenz LL, and Harris RA. A Breakthrough: Macrophage-Directed Cancer Immunotherapy. *Cancer Res* 2016; 76: 513-516.

50. Pyonteck SM, Akkari L, Schuhmacher AJ, Bowman RL, Sevenich L, Quail DF et al. CSF-1R inhibition alters macrophage polarization and blocks glioma progression. *Nat Med* 2013; 19: 1264-1272.
51. Quail DF, Bowman RL, Akkari L, Quick ML, Schuhmacher AJ, Huse JT et al. The tumor microenvironment underlies acquired resistance to CSF-1R inhibition in gliomas. *Science* 2016; 352: DOI: 10.1126/science.aad3018.

Figure legends

Fig. 1. Macrophage secreted factors directly induce chemoresistance and activate Insulin/ IGF1 receptors in pancreatic cancer cells

(A) Left: Human pancreatic SUIT-2 cancer cells were cultured in the presence or absence of macrophage conditioned media (MCM) from human primary macrophages, and treated with 200 nM gemcitabine for 24 hours or left untreated. Percentage of cell death was quantified by flow cytometry. Error bars represent s.d. (n=4); two tailed unpaired t-test; *** $p \leq 0.005$.

Right: Mouse primary KPC-derived pancreatic cancer cells were cultured in the presence or absence of MCM from mouse primary macrophages, and treated with 200 nM gemcitabine for 24 hours or left untreated. Percentage of cell death was quantified by flow cytometry. Error bars represent s.d. (n=3); two tailed unpaired t-test; * $p \leq 0.05$.

(B) Human pancreatic cancer SUIT-2 cells were serum starved for 24 hours and exposed for 2 hours to human MCM, or left unexposed, and protein lysates were subjected to a phospho-receptor tyrosine kinase array. Number 1, shows phospho-Insulin receptor, number 2, phospho-AXL receptor and number 3, phospho- Ephrin receptor. **(C)** Immunoblotting analysis of phospho-Insulin/IGF1 receptors, Insulin receptor, IGF1 receptor and tubulin in SUIT-2 cells serum starved or exposed to MCM for 30 minutes or 3 hours. **(D)** Immunoblotting analysis of pan-phospho tyrosine, Insulin receptor and IGFR1 in Insulin and IGFR1 immunoprecipitates of SUIT-2 cells treated with human MCM for 3 hours or left untreated. **(E)** Quantification of *Igf-1*, *Igf-2* and *Insulin* mRNA expression levels in human primary macrophages (n=3). **(F)** Quantification of *Igf-1*, *Igf-2* and *Insulin* mRNA expression levels in mouse primary

macrophages (n=3). **(G)** Immunoblotting analysis of IGF1 and IGF2 ligands in human and mouse MCM and macrophage lysates. **(H)** Immunoblotting analysis of phospho-Insulin/IGF1 receptor, Insulin receptor, IGFR1 and tubulin, in human pancreatic cancer SUIT-2 cells and murine primary KPC- derived pancreatic cancer cells serum starved, exposed to MCM or exposed to recombinant IGF for 3 hours.

Fig. 2. Blockade of IGF impairs macrophage-mediated chemoresistance of pancreatic cancer cells

(A) Immunoblotting analysis of SUIT-2 cells untreated or treated with MCM or MCM+IGF blocking antibody for 3 hours. **(B)** Quantification of cell death in SUIT-2 cells treated with gemcitabine, MCM and IGF blocking antibody for 24 hours. Error bars represent s.d. (n=3); ** $p \leq 0.01$ and * $p \leq 0.05$ using one-way ANOVA and Tukey's post hoc test. **(C)** Quantification of cells death in primary mouse KPC-derived pancreatic cancer cells untreated or treated with gemcitabine, MCM, IGF blocking antibody or recombinant IGF for 24 hours. Error bars represent s.d. (n=3); *** $p \leq 0.005$ using one-way ANOVA and Tukey's post hoc test. **(D)** Representative flow cytometry dot blots of KPC-derived cells exposed to gemcitabine, MCM, IGF blocking antibody and recombinant IGF. **(E)** Immunoblotting analysis of PARP and tubulin in human SUIT-2 pancreatic cancer cells and cleaved caspase-3 and tubulin in KPC-derived mouse pancreatic cancer cells untreated, treated with gemcitabine, MCM + gemcitabine or recombinant IGF + gemcitabine for 24 hours. **(F)** Quantification of cell death in KPC-derived cells cultured in the presence or absence of MCM or recombinant IGF and treated with 10, 100 or 1000 nM nab-paclitaxel for 36 hours. Error bars represent s.d. (n=3); *** $p \leq 0.005$, ** $p \leq 0.01$ using one-way ANOVA and Tukey's post hoc test.

Fig. 3. Insulin and IGF1 receptors are activated on cancer cells in biopsies from PDA patients, and this correlates with increased numbers of TAMs

(A) Left: Confocal microscopy images of frozen human PDA tissues immunofluorescently co-stained for the tumor epithelial marker CK11 (in green), phospho-Insulin/IGF1 receptors (in red), and nuclei (in blue). Scale bar, 100 μm . **Right:** Immunohistochemical staining of phospho-Insulin/IGF1 receptors in normal human pancreas and biopsies from PDA patients. Scale bars, 100 μm and 50 μm . **(B)** Images of normal and malignant human pancreatic ducts immunohistochemically stained for phospho-Insulin/IGF1 receptors. Scale bar, 50 μm . **(C)** Pie diagram representing the percentage of phospho-Insulin/IGF1 receptor positive (red) and negative (green) tumors assessed in tissue microarrays (TMA) containing biopsies from 53 consented PDA patients. **(D) Left:** Confocal microscopy images of frozen human PDA tissues immunofluorescently co-stained for CD68 (green), CK19 (red) and nuclei (blue). Scale bar, 100 μm . **Right:** Immunohistochemical staining of CD163 in normal human pancreas and biopsies from PDA patients. Scale bars, 100 μm and 50 μm . **(E)** Serial sections of biopsies from human PDA samples immunohistochemically stained for phospho-Insulin/IGF1 receptors and CD163. Scale bar, 50 μm . **(F)** Contingency table and results from statistical analysis showing a strong evidence of positive correlation between phospho-Insulin/IGF1R expression in tumors and increased CD163+ macrophage infiltration. Relative risk = 4.92 (95% CI- [1.82 – 13.34]), $p = 0.001$ using Fisher exact test. **(G)** Immunofluorescent images of human PDA tissues stained for CD68 (in green), IGF-1 or IGF-2 (in red) and nuclei (in blue). White stars indicate CD68+ macrophages that express IGF-1 or IGF-2. Scale bar, 50 μm .

Fig.4. TAMs and myofibroblasts are major sources of IGF-1 and IGF-2 in pancreatic tumors

(A) KPC-derived tumor cells were orthotopically implanted into the pancreas of syngeneic recipient mice. Images show hematoxylin and Eosin (H&E), CD206 and phospho-Insulin/IGF1 receptors staining of naïve mouse pancreas and murine PDA tissue samples harvested 29 days after tumor implantation. **(B)** Normal pancreas from naïve mice and

pancreatic tumors were harvested and digested on day 29 after implantation. Percentage of intra-tumoral F4/80+ macrophages, Gr1+/CD11b+ neutrophils and myeloid derived suppressor cells (MDSCs), CD4+ and CD8+ T cells, among CD45+ immune cells, were quantified by flow cytometry (n= 2 normal pancreas; n= 4 pancreatic carcinomas). **(C)** Quantification of *Igf-1* and *Igf-2* mRNA expression levels in F4/80+ and F4/80- cells isolated from pancreatic tumors. Error bars represent s.d. (n=3). **(D)** KPC^{luc/zsGreen} (zsGreen) -derived tumor cells (FC1242^{luc/zsGreen}) were orthotopically implanted into the pancreas of syngeneic recipient (C57/BL6) mice. Tumors were harvested and digested at day 23 after implantation and tumor cells, non-immune stromal cells, M1-like and M2-like macrophages were sorted by flow cytometry. **(E)** Dot-blot showing F4/80+/CD206+ and F4/80+/CD206- intra-tumoral macrophages (left) and the percentage of F4/80+/CD206- M1-like macrophages and F4/80+/CD206+ M2-like macrophages in pancreatic tumors (right). **(F)** Quantification of *Igf-1* (Left) and *Igf-2* (right) mRNA expression levels in CD45+/F4/80+/CD206- M1-like macrophages, CD45+/F4/80+/CD206+ M2-like macrophages, CD45-/zsGreen- non-immune stromal cells and CD45-/zsGreen+ tumor cells isolated from murine pancreatic tumors. Error bars represent s.d. (n=3).

Fig. 5. Combination of gemcitabine with IGF blocking antibody BI 836845 inhibits tumor growth in a syngeneic orthotopic pancreatic cancer model.

(A) KPC^{luc/zsGreen} (zsGreen) -derived pancreatic tumor cells (FC1242^{luc/zsGreen}) were orthotopically implanted into the pancreas of syngeneic C57BL/6 recipient mice, and mice were treated, starting at day 7 after tumor implantation, twice a week i.p., with either control IgG antibody, gemcitabine (100 mg/Kg), IGF blocking antibody BI 836845 (100 mg/Kg) or a combination of gemcitabine with BI 836845. **(B)** Representative images of tumors and tumor weights are shown (n= 6 mice per group); * p ≤ 0.05 using one-way ANOVA and Tukey's post-hoc test. **(C)** Pancreatic tumors were digested and percentage of intra-tumoral F4/80+ macrophages, Ly6C+/Ly6G- inflammatory monocytes, Gr1+/CD11b+ neutrophils and myeloid derived suppressor cells (MDSCs), and CD8+ cytotoxic T cells (CTLs), among

CD45+ immune cells, were quantified by flow cytometry. **(D)** Percentage of intra-tumoral CD206- M1-like macrophages and CD206+ M2-like macrophages, among F4/80+ macrophages, were quantified by flow cytometry. **(E)** Immunohistochemical staining of phospho-Insulin/IGF1R and cleaved caspase-3 in pancreatic tumors treated with IgG (control), gemcitabine, IGF blocking antibody BI 836845 or gemcitabine + BI 836845. **(F)** Quantification of cleaved caspase-3 positive dead cells in tumors treated with IgG (control), gemcitabine, IGF blocking antibody BI 836845 or gemcitabine + BI 836845 (8-11 fields counted/ mouse tumor), *** $p \leq 0.005$ compared to other treatment groups, using one-way ANOVA and Tukey's post-hoc test.

Fig.6. Combination of gemcitabine with IGF blocking antibody ab9572 decreases tumor growth in a syngeneic orthotopic pancreatic cancer model.

(A) Primary mouse KPC-derived pancreatic cancer cells were implanted orthotopically in the pancreas of syngeneic recipient mice. Mice were administered i.p., twice a week with IgG antibody, gemcitabine alone or gemcitabine with an IGF blocking antibody from abcam (ab9572). Tumors were harvested at day 30 and representative images are shown. **(B)** Tumor weights are shown (n=9-12 mice per group). ** $p \leq 0.01$, * $p \leq 0.05$ using one-way ANOVA and Tukey's post-hoc test. **(C) Left**, Immunohistochemical staining of phospho-Insulin/IGF1R, and cleaved caspase-3 in pancreatic tumors treated with IgG, gemcitabine or gemcitabine+ IGF blocking antibody ab9572. **Right**, Quantification of cleaved caspase-3 positive dead cells in pancreatic tumors from mice treated with IgG control antibody, gemcitabine or gemcitabine+ ab9572 IGF blocking antibody (6-8 fields counted/mouse tumor), ** $p \leq 0.01$ using one-way ANOVA and Tukey's post-hoc test. **(D)** Schematics depicting the role of stroma-derived IGF in activation of the Insulin/IGF1R signaling survival pathway, and in mediating chemoresistance of pancreatic cancer cells.

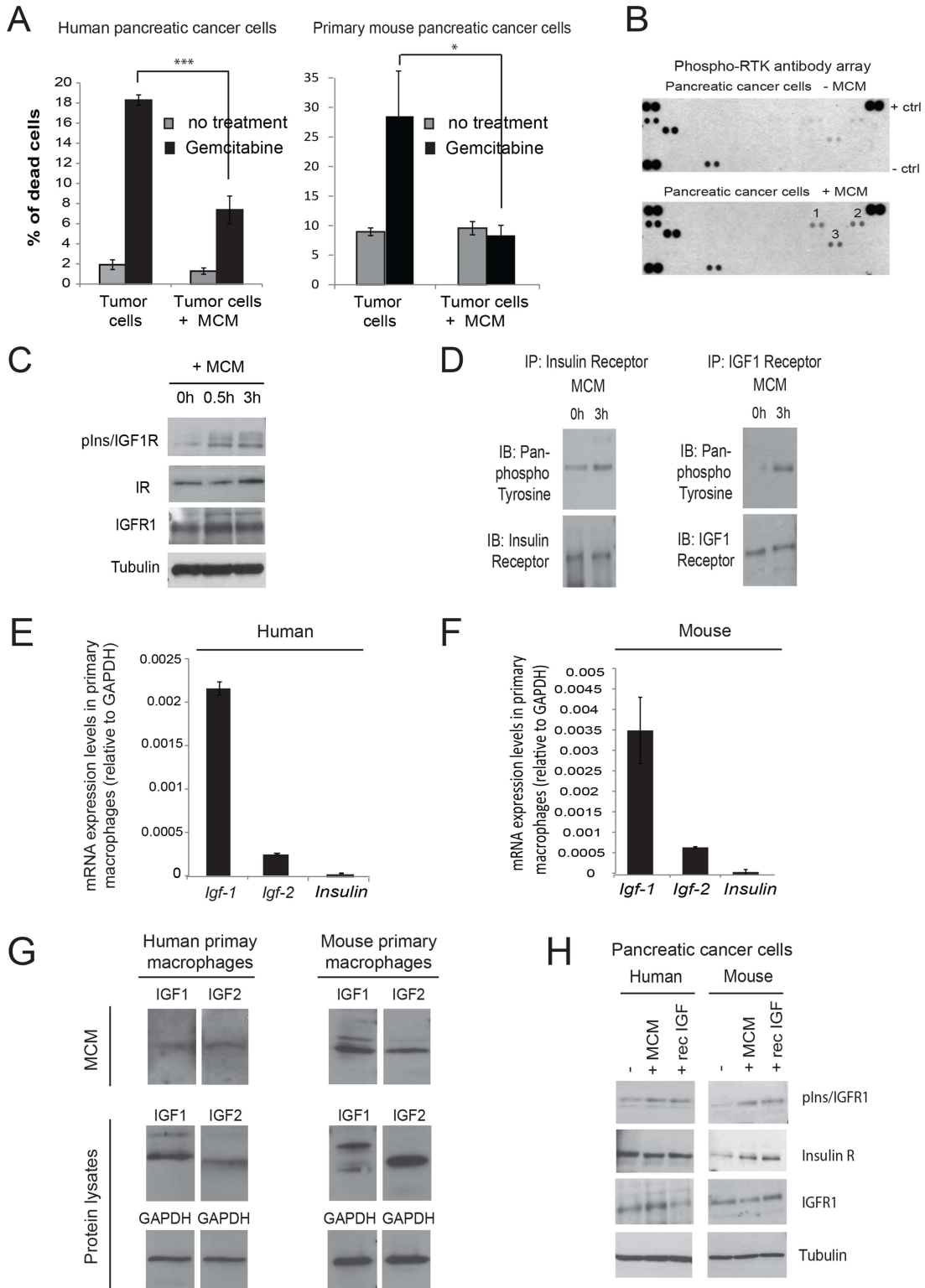


Figure 1

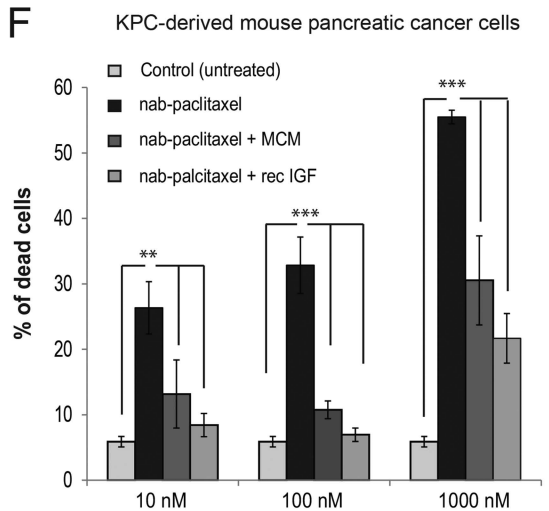
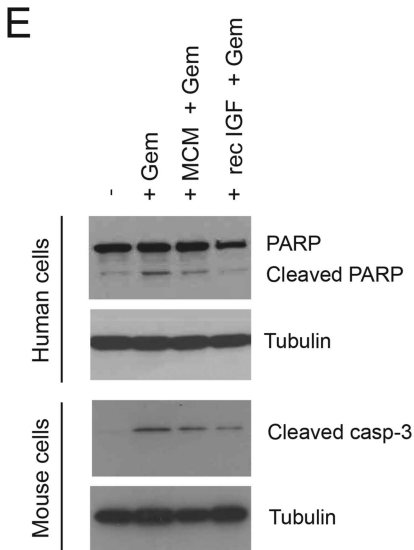
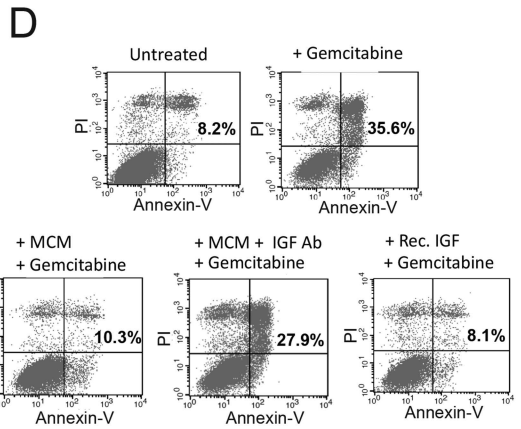
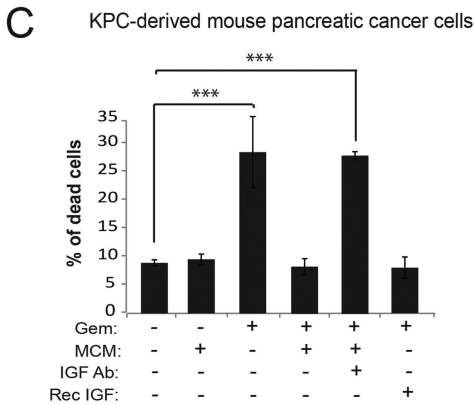
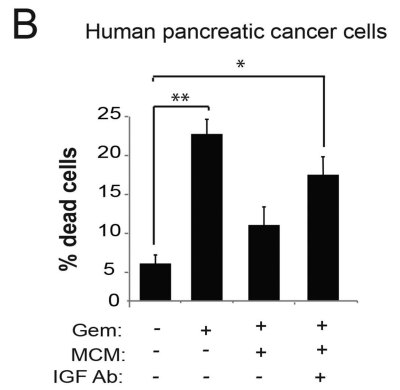
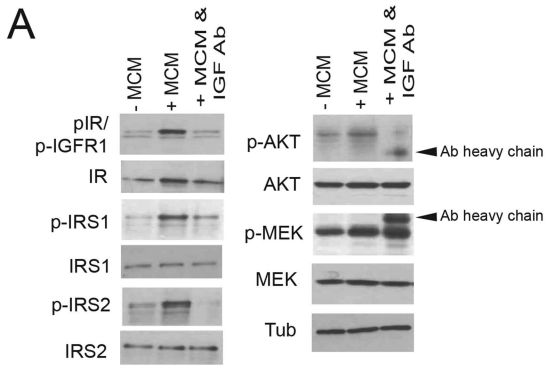


Figure 2

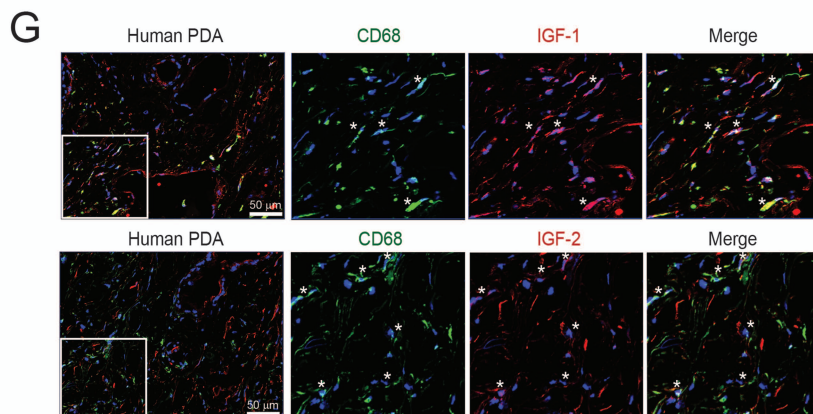
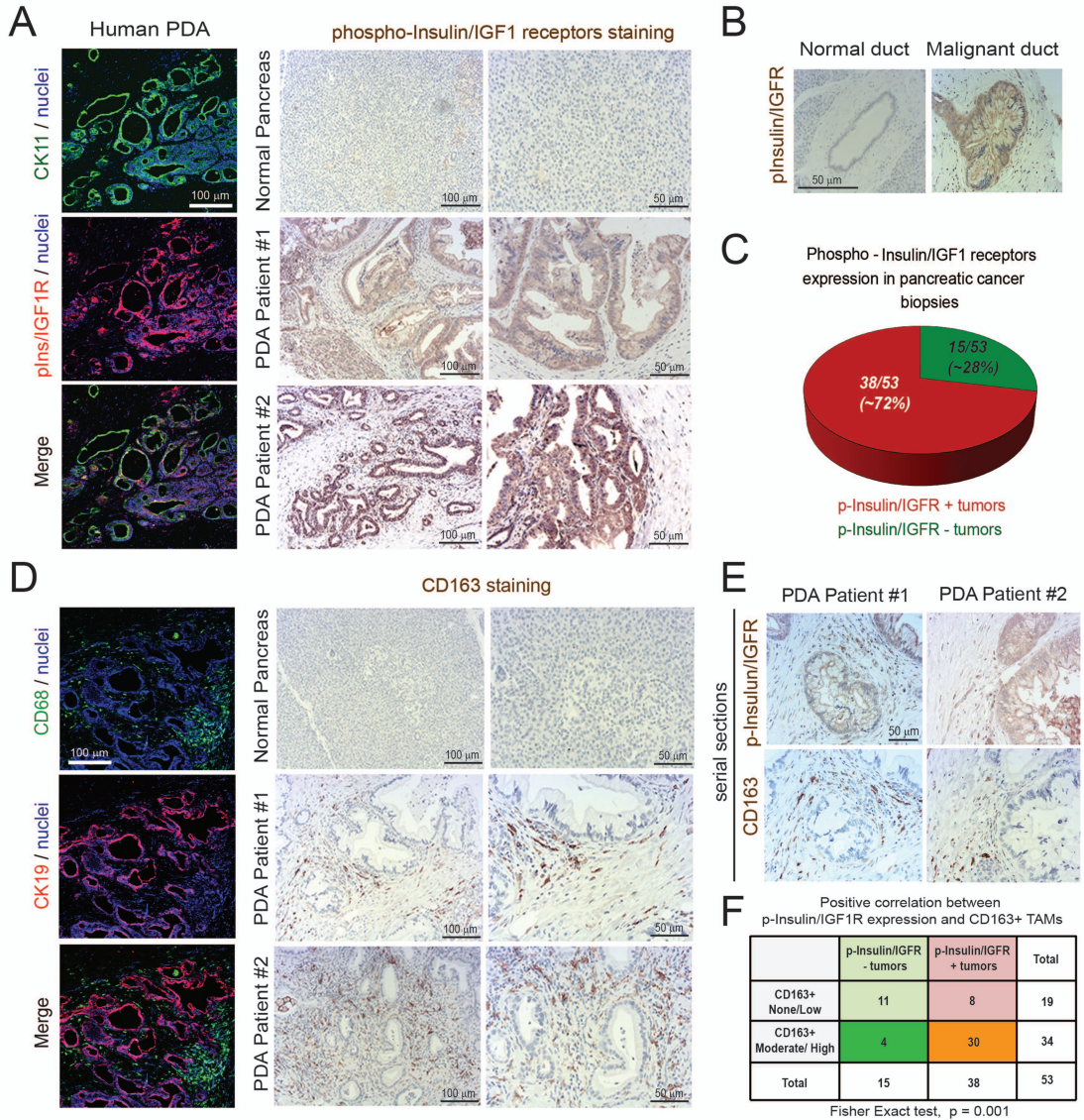


Figure 3

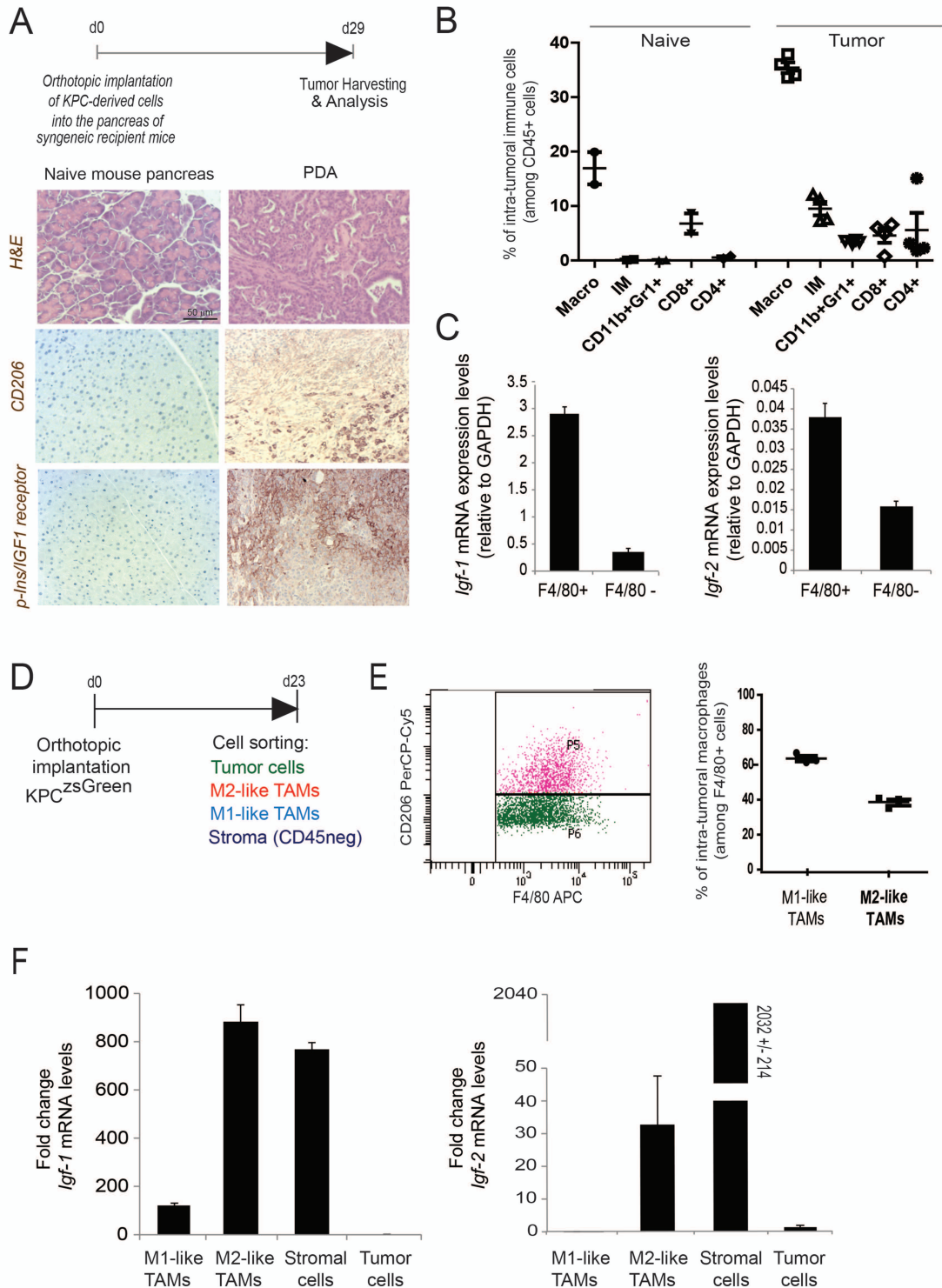
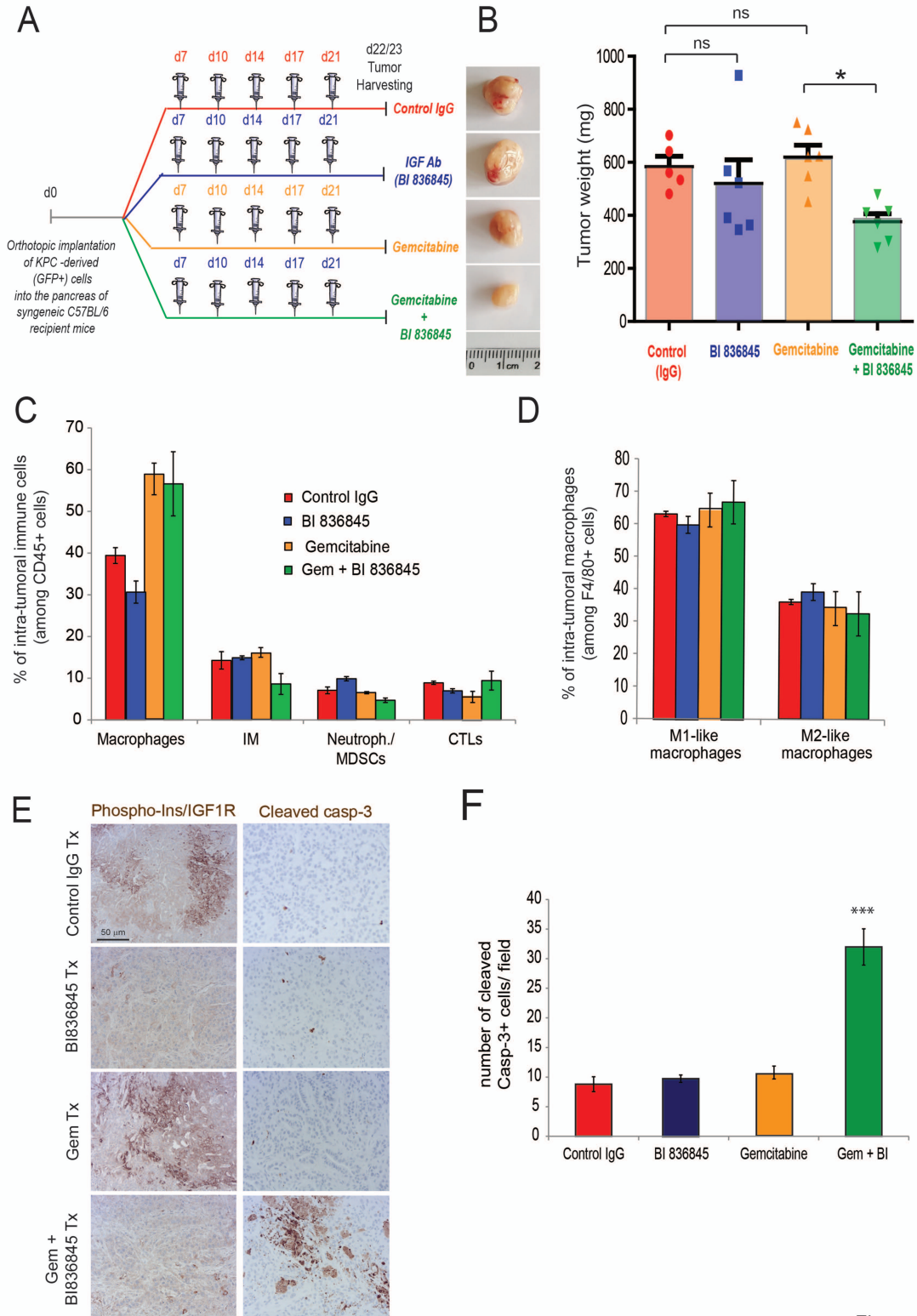


Figure 4



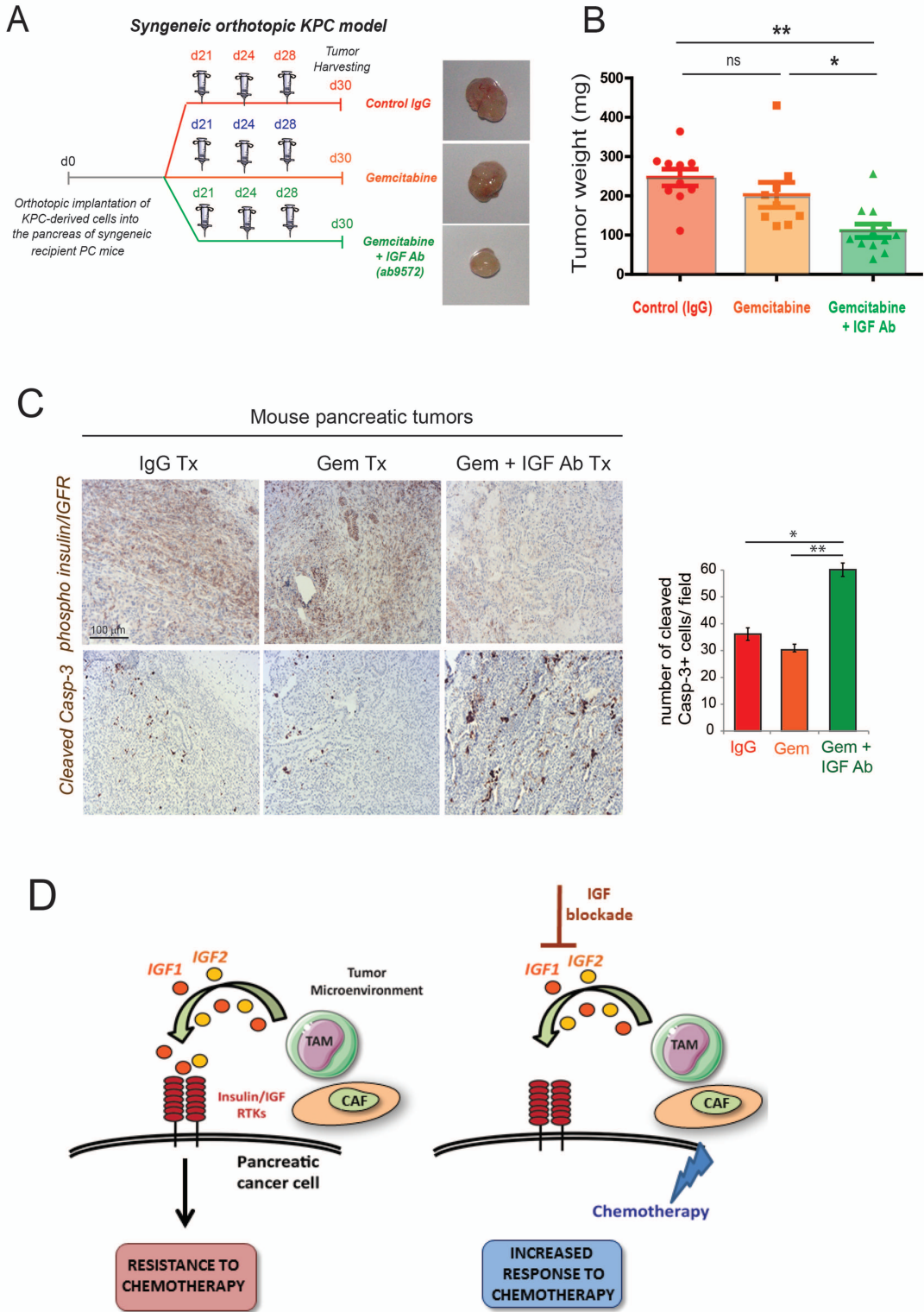


Figure 6

Supplementary Data

Supplementary Figure legends

Fig. S1. Primary M2-like macrophages express IGF-1 and IGF-2

(A) *CD206* and *IL-12* mRNA expression levels were quantified in primary human macrophages that were generated using macrophage colony-stimulating factor 1 (M-CSF1) and polarized into M1 macrophages (IFN γ + LPS) or M2 macrophages (IL-4) (n=3). **(B)** *CD206* and *IL-12* mRNA expression levels were quantified in primary murine macrophages that were generated using macrophage colony-stimulating factor 1 (M-CSF1) and polarized into M1 macrophages (IFN γ + LPS) or M2 macrophages (IL-4) (n=3). **(C)** Quantification of *Igf-1* and *Igf-2* mRNA expression levels in primary human macrophages polarized into M1 macrophages or M2 macrophages (n=3). **(D)** Quantification of *Igf-1* and *Igf-2* mRNA expression levels in primary murine macrophages polarized into M1 macrophages or M2 macrophages (n=3). **(E)** Quantification of *Igf-1*, *Igf-2* and *Insulin* mRNA expression levels in mouse primary macrophages and KPC-derived tumor cells (n=3).

Fig. S2. In the absence of chemotherapy, addition of MCM, IGF blockade or recombinant IGF does not affect proliferation or survival of pancreatic cancer cells.

(A) Quantification of cell death in SUIT-2 cells treated with gemcitabine, MCM and IGF blocking antibody for 24 hours. Error bars represent s.d. (n=3); * $p \leq 0.05$, two tailed unpaired t-test. **(B)** Cell cycle analysis of primary mouse KPC derived pancreatic cancer cells exposed to MCM, IGF blocking antibody (10 μ g/ml) or recombinant IGF (100 ng/ml).

Fig.S3. MCM enhances resistance of pancreatic cancer cells to gemcitabine, 5-FU and paclitaxel in an IGF-dependent manner.

(A) Quantification of cell death in human SUIT-2, MIA-PaCa-2 and murine KPC-derived pancreatic cancer cells treated with gemcitabine, MCM and IGF blocking antibody for 24 hours. **(B)** Quantification of cell death in SUIT-2, MIA-PaCa-2 and KPC-derived pancreatic cancer cells treated with paclitaxel, MCM and IGF blocking antibody for 24 hours. **(C)** Quantification of cell death in SUIT-2, MIA-PaCa-2 and KPC-derived pancreatic cancer cells treated with 5-FU, MCM and IGF blocking antibody for 24 hours. Error bars represent s.e (n=3), *** $p \leq 0.005$, ** $p \leq 0.01$, * $p \leq 0.05$ compared to control using one-way ANOVA and Tukey's post-hoc test.

Fig. S4. Biopsies from pancreatic cancer patients express activated Insulin and IGF1 receptors and are infiltrated by macrophages.

(A) Confocal microscopy images of frozen human PDA biopsies immunofluorescently co-stained for CK11 (green), phospho-Insulin/IGF1 receptor (red) and nuclei (blue). Scale bar, 50 μm . **(B)** Immunohistochemical staining of phospho-Insulin receptor (left) and phospho-IGF1 receptor (right) in serial sections of biopsies from PDA patients. Scale bar, 50 μm . **(C)** Immunohistochemical staining of phospho-Insulin/IGF1 receptor, CD163 and CD68 in human normal pancreas and serial sections of biopsies from PDA patients. **(D)** Quantification of CD68+ and CD163+ macrophages in human normal pancreas and PDA samples (n= 6 fields). Error bars represent s.d. (n=6); two tailed unpaired t-test, *** $p \leq 0.005$.

Fig. S5. Mouse orthotopic pancreatic tumors are rich in macrophages and myofibroblasts.

(A) Immunohistochemical staining of αSMA and CD68 in paraffin embedded tissues from naïve mouse pancreas and mouse pancreatic tumors. Scale bar, 50 μm . **(B)** Immunofluorescent staining of EpCAM (green), αSMA (red) and nuclei (blue) in frozen tissues from naïve mouse pancreas and mouse pancreatic tumors. Scale bar, 100 μm .

Fig. S6. Tumors from KPC mouse model express activated Insulin/IGF1 receptors.

Immunohistochemical staining of phospho-Insulin/IGF1 receptors, CD206 and α SMA in serial sections of PDA tissues from the genetically engineered KPC mouse model, and in adjacent normal pancreas. Scale bar, 50 μ m.

Fig. S7. Gating strategy used to FACS-sort tumor cells, immune cells and stromal cells.

(A) Gating strategy used to sort CD45-/zsGreen+ KPC-derived tumor cells, CD45-/zsGreen- non immune stromal cells, CD45+F4/80+/CD206- macrophages and CD45+/F4/80+/CD206+ macrophages from mouse pancreatic tumors. **(B)** Quantification of α SMA mRNA expression levels in the CD45-/zsGreen- non immune stromal cell population isolated from pancreatic tumors using flow cytometry (n=3).

Fig. S8. Primary pancreatic myofibroblasts secrete IGF-1 and IGF-2.

(A) Light microscopy image and Immunoblotting analysis of α SMA and GAPDH in mouse primary pancreatic myofibroblasts. **(B)** Quantification of *Igf-1* and *Igf-2* mRNA expression levels in pancreatic myofibroblasts exposed or unexposed to KPC-derived tumor conditioned media (TCM). **(C)** Immunoblotting analysis of IGF1 and IGF2 ligands in pancreatic myofibroblast conditioned media (MyoCM) and myofibroblast lysates. **(D)** Quantification of cell death in KPC-derived pancreatic cancer cells treated with gemcitabine, paclitaxel or 5-FU, myofibroblast conditioned media (MyoCM) and IGF blocking antibody for 24 hours. Error bars represent s.e (n=3), , *** $p \leq 0.005$, ** $p \leq 0.01$, * $p \leq 0.05$ compared to control using one-way ANOVA and Tukey's post-hoc test.

Fig. S9. IGF-1 and IGF-2 are expressed in the tumor microenvironment of PDA patients.

Immunohistochemical staining of IGF-1, IGF-2, CD163 and α SMA in serial sections of a biopsy from PDA patient. Scale bars, 50 μ m and 100 μ m.

Fig. S10. Gating strategies used to analyse tumor infiltrated immune cell populations.

Gating strategies used to analyze CD45+/F4/80+/CD206- macrophages and, CD45+/F4/80+/CD206+ macrophages, CD45+/CD11b+/Ly6C+/Ly6G- inflammatory monocytes, CD45+/CD11b+/Gr1+ neutrophils and MDSCs, and CD45+/CD4+ and CD45+/CD8+ T cells from mouse pancreatic tumors by flow cytometry.

Fig. S11. IGF blockade decreases activation of Insulin and IGF1 receptors in pancreatic tumors.

Immunohistochemical staining of phospho-Insulin receptor (top) and phospho-IGF1 receptor (bottom) in control (IgG) treated mouse pancreatic tumors, and tumors treated with IGF blocking antibodies BI 836845 and ab 9572. Scale bar, 50 μ m.

Fig. S12. Combination of 5-FU and paclitaxel with BI 836845 in a syngeneic orthotopic pancreatic cancer model.

(A) KPC^{luc/zsGreen}-derived pancreatic tumor cells were orthotopically implanted into the pancreas of syngeneic C57BL/6 recipient mice, and mice were treated, starting at day 6 after tumor implantation, twice a week i.p., with either control IgG antibody, 5-FU (50 mg/Kg), paclitaxel (10 mg/Kg), a combination of 5-FU with BI 836845 (100 mg/Kg) or a combination of paclitaxel with BI 836845. **(B)** Tumor weights (n=6 mice per group); p values obtained using unpaired two tailed T-test. **(C)** Immunohistochemical staining of phospho-Insulin/IGF1R and cleaved caspase-3 in pancreatic tumors treated with IgG (control), 5-FU, 5-FU + BI 836845, paclitaxel, and paclitaxel + BI 836845. Scale bar, 50 μ m. **(D)** Quantification of cleaved caspase-3 positive dead cells in tumors treated with IgG (control), 5-FU, 5-FU + BI 836845, paclitaxel, and paclitaxel + BI 836845 (3-5 fields counted/ tumor tissues from 5-6 mice per treatment group), * p \leq 0.05 using unpaired two tailed T-test.

Supplementary Tables

PDA patient samples from U.S. Biomax (Pa483c)

position	sex	age	organ	pathology	grade	stage	tnm
A1	F	77	Pancreas	Duct adenocarcinoma	1	IB	T2N0M0
A2	F	47	Pancreas	Duct adenocarcinoma (ductal ectasia)	-	IIA	T3N0M0
A3	F	64	Pancreas	Duct adenocarcinoma (fibrofatty tissue)	-	I	T2N0M0
A4	M	77	Pancreas	Duct adenocarcinoma	1	IB	T2N0M0
A5	F	67	Pancreas	Duct adenocarcinoma	1	IIB	T3N1BM0
A6	M	34	Pancreas	Duct adenocarcinoma	1	II	T3N0M0
A7	F	56	Pancreas	Duct adenocarcinoma	1	IB	T2N0M0
A8	M	74	Pancreas	Duct adenocarcinoma	1	IIA	T3N0M0
B1	F	72	Pancreas	Duct adenocarcinoma	2	IIA	T3N0M0
B2	M	49	Pancreas	Duct adenocarcinoma	1	IIB	T3N1M0
B3	M	39	Pancreas	Duct adenocarcinoma	2	IIA	T3N0M0
B4	F	54	Pancreas	Duct adenocarcinoma	1	IB	T2N0M0
B5	F	48	Pancreas	Duct adenocarcinoma	1	IIA	T3N0M0
B6	F	76	Pancreas	Duct adenocarcinoma	2	IIA	T3N0M0
B7	M	57	Pancreas	Duct adenocarcinoma	2	IIA	T3N0M0
B8	M	42	Pancreas	Duct adenocarcinoma (fibrous tissue)	-	IIA	T3N0M0
C1	M	47	Pancreas	Duct adenocarcinoma	2	IIA	T3N0M0
C2	M	31	Pancreas	Duct adenocarcinoma	2	IIA	T3N0M0
C3	M	64	Pancreas	Duct adenocarcinoma	3	IIA	T3N0M0
C4	M	44	Pancreas	Duct adenocarcinoma	2	II	T3N0M0
C5	M	57	Pancreas	Duct adenocarcinoma	2	IIA	T3N0M0
C6	M	61	Pancreas	Duct adenocarcinoma	2	IB	T2N0M0
C7	M	65	Pancreas	Duct adenocarcinoma	2	IIA	T3N0M0
C8	M	52	Pancreas	Duct adenocarcinoma (sparse)	2	IA	T1N0M0
D1	M	49	Pancreas	Duct adenocarcinoma	2	IIA	T3N0M0
D2	F	47	Pancreas	Duct adenocarcinoma	3	IIB	T3N1M0
D3	M	45	Pancreas	Duct adenocarcinoma	2	IIA	T3N0M0
D4	M	60	Pancreas	Duct adenocarcinoma	2	II	T3N0M0
D5	M	52	Pancreas	Adenocarcinoma	3	IB	T2N0M0
D6	F	62	Pancreas	Adenocarcinoma	3	II	T3N0M0
D7	F	51	Pancreas	Adenocarcinoma	3	IIA	T3N0M0
D8	F	48	Pancreas	Adenocarcinoma	3	IIA	T3N0M0
E1	M	61	Pancreas	Adenocarcinoma	3	IV	T3N0M1
E2	M	78	Pancreas	Adenocarcinoma	3	IIA	T3N0M0
E3	M	52	Pancreas	Duct adenocarcinoma	2	IA	T2N0M0
E4	M	56	Pancreas	Adenocarcinoma	3	IA	T2N0M0
E5	F	51	Pancreas	Adenocarcinoma	3	IIA	T3N0M0
E6	F	56	Pancreas	Adenocarcinoma	3	IIA	T3N0M0
E7	F	66	Pancreas	Acinic cell carcinoma	-	IB	T2N0M0
E8	M	62	Pancreas	Squamous cell carcinoma	2	IIA	T3N0M0

- pInsulin/IGFR - / CD163 -
- pInsulin/IGFR - / CD163 +
- pInsulin/IGFR + / CD163 -
- pInsulin/IGFR + / CD163 +

Table S1. Clinical information from 40 consented PDA patient samples.

Clinical information from 40 consented PDA patient samples from U.S. Biomax, analyzed for phospho-Insulin/IGF1R expression on cancer cells and CD163+ macrophages.

PDA patient samples from Liverpool tissue bank

Number	Diagnosis	T stage	N stage	M stage	Gender	Age at surgery
1	PDA	2	1	x	Male	63
2	PDA	unrecorded	unrecorded	unrecorded	Female	54
3	PDA	3	1	x	Female	80
4	PDA	Unrecorded	Unrecorded	Unrecorded	Male	70
5	PDA	3	1	x	Male	68
6	PDA	1	0	x	Male	65
7	PDA	3	1	x	Female	52
8	PDA	3	0	x	Female	64
9	PDA	3	1	X	Male	58
10	PDA	3	1	x	Male	70
11	PDA	3	1	x	Female	57
12	PDA	Unrecorded	Unrecorded	Unrecorded	Female	69
13	PDA	3	1	x	Male	60
14	PDA	3	1	x	Male	55
15	PDA	3	1	x	Male	52
16	PDA	3	1	x	Male	71

- pInsulin/IGFR - / CD163 -
- pInsulin/IGFR - / CD163 +
- pInsulin/IGFR + / CD163 -
- pInsulin/IGFR + / CD163 +

Table S2. Clinical information from 16 consented PDA patient samples.

Clinical information from 16 consented PDA patient samples from the Liverpool tissue bank, analyzed for phospho-Insulin/IGFR expression on cancer cells and CD163+ macrophages.

Supplementary Materials & Methods

Generation of primary KPC-derived pancreatic cancer cells and cell culture conditions

The murine pancreatic cancer cells KPC FC1242 were generated in the Tuveson lab (Cold Spring Harbor Laboratory, New York, USA) isolated from PDA tumor tissues obtained from LSL-Kras^{G12D}; LSL-Trp53^{R172H}; Pdx1-Cre mice of a pure C57BL/6 background. Briefly, a fragment of 3mm³ of PDA was excised, washed in 10 ml PBS, and then finely diced with sterile razors. Cells were incubated in 10 ml collagenase type V solution (2 mg/ml in DMEM) at 37°C for 45 minutes with mixing. Cells were centrifuged (300 x g) and resuspended in DMEM + 10% FBS + Penicillin/Streptomycin and plated in tissue culture treated plates. Cells were initially split at high dilutions (1:20 to 1:100) to dilute out our stromal cell contamination, which do not tolerate aggressive splitting, whereas the cancer cells formed ductal-like colonies.

KPC cells were isolated in our laboratory from PDA tumor tissues obtained from LSL-Kras^{G12D}; LSL-Trp53^{R172H}; Pdx1-Cre mice in the mixed 129/SvJae/C57Bl/6 background as described previously [35]. Briefly, a 3mm³ fragment of PDA was excised, washed in 10 ml PBS, and then finely diced with sterile razors. Cells were incubated in 10 ml collagenase type V solution (1mg/ml in DMEM/F12) at 37°C for 30-45 minutes with mixing. Cells were centrifuged (300 x g) and resuspended in 0.05% Trypsin/EDTA for 5 min at 37C. Digest was quenched by adding DMEM+ 10% fetal bovine serum and 96 uM CaCl₂. Cells were washed 3 times with DMEM/F12 medium and plated in Biocoat dishes (Collagen I). Cells were maintained on collagen coated plates at a minimal passage number (< p8) to allow initial expansion prior to use for *in vitro* and *in vivo* experiments.

Macrophage polarization

Polarization to M1 macrophages was performed using 20 or 50 ng/ml INF γ (Peprotech) and 100 or 10 ng/ml LPS (Sigma Aldrich) for murine or human macrophages respectively.

Polarization to M2 was performed using 20 or 40 ng/ml IL-4 ng/ml for murine or human macrophages respectively.

Cell cycle analysis

KPC derived pancreatic cancer cells were treated with isogenic mouse MCM, IGF blocking antibody (abcam 9572) at 10 µg/ml or recombinant IGF (Peprotech 100-11) at 100ng/ml. Cells were harvested, fixed with methanol, treated for 45 min with 10 µg/ml of RNase, resuspended in PBS containing 10 µg/ml of propidium iodide and subjected to flow cytometry.

Immunohistochemical analysis

Deparaffinization and antigen retrieval was performed using an automated DAKO PT-link. Paraffin-embedded human and mouse PDA tumors were immunostained using the DAKO envision+ system-HRP. Tissue sections were incubated for 1 hour at room temperature with primary antibodies against phospho-Insulin/IGF1 receptors (R&D, AF2507, used 1:50 after high pH antigen retrieval), phospho Insulin receptor (LS Bio, LS-C177981, used 1:100 after low pH antigen retrieval), phospho-IGF1 receptor (Biorbyt, orb97626, used 1:100 after high pH antigen retrieval), CD68 (DAKO, clone KP1, M081401-2 used 1:2000 after high pH antigen retrieval), CD163 (abcam, ab74604 pre-diluted after low pH antigen retrieval), αSMA (abcam, Ab 5694 used 1:100 after low pH antigen retrieval), CD206 (abcam, ab8919 used 1:50 after low pH antigen retrieval), IGFs (abcam, ab9572 and ab9574 used at 1: 200 after high and low pH antigen retrieval respectively), cleaved caspase-3 (cell signaling #9661 used at 1:300 after high pH antigen retrieval) followed by secondary-HRP conjugated antibody (from DAKO envision kit) for 30 minutes at room temperature. All antibodies were prepared in antibody diluent from Dako envision kit. Staining was developed using diaminobenzidine and counterstained with hematoxylin.

Analysis and scoring of tissues were performed by a pathologist, and statistical significance was independently determined by a biostatistician. Both experts worked in a blinded fashion.

Immunofluorescence

Human and mouse PDA frozen tissue sections were fixed with cold acetone, permeabilized in 0.1% Triton, blocked in 8% goat serum and incubated overnight at 4°C with anti-phospho Insulin/IGF1R (R&D) (1:200), CD68 (DAKO, clone KP1) (1:200), CK19 (abcam) (1:200), CK11 (Cell signaling) (1:200), IGFs (abcam) (1:200), α SMA (abcam) (1:100), EpCAM (BD Pharmingen) (1:100).

Immunoprecipitation and Immunoblotting

Immunoprecipitation was performed using anti-Insulin (abcam, 137747) and anti-IGFR1 (R&D, AF305-NA) overnight at 4°C.

Immunoblotting analysis were performed using the following primary antibodies overnight at 4°C: anti-phospho Insulin/pIGFR1 (R&D AF2507, 1:400 in 5% Milk-TBST), anti-tubulin (Sigma T6199, 1:5000 in 2.5% BSA-TBST), anti-Insulin (abcam 137747, 1:1000 in 2.5% BSA-TBST), anti-IGF1R (R&D AF305-NA, 1:1000 in 2.5% BSA-TBST), anti-pan phospho tyrosine (Merck Millipore 05-321X, 1:1000 in 2.5% BSA-TBST), anti-IGFs (abcam 9572, 1:500 in 2.5% BSA-TBST and abcam 9574, 1:1000 in 5% Milk-TBST), GAPDH (Sigma, G9545, 1:10,000 in 2.5% BSA-TBST), anti-cleaved caspase 3 (Cell signalling 9661, 1:1000 in 5% Milk-TBST), anti-PARP (BD 556494, 1:1000 in 2.5% BSA-TBST), anti-phospho-IRS1 (Millipore 09-432, 1:1000 in 2.5% BSA-TBST), anti-IRS1 (Cell Signaling 2382S, 1:1000 in 5% BSA-TBST), anti-phospho-IRS2 (Biorbyt orb34833, 1:500 in 2.5% BSA-TBST) anti-IRS2 (Cell Signaling 4502s, 1:1000 in 5% BSA-TBST), anti-phospho-AKT (Cell Signaling 4060, 1:1000 in 2.5% BSA-TBST), anti-AKT (Cell Signaling 9272, 1:1000 in 2.5% BSA-TBST), anti-phospho-MEK (Cell Signaling 2338s, 1:1000 in 5% BSA-TBST), anti-MEK (Cell Signaling 9126s, 1:1000 in 5% BSA-TBST).

Syngeneic Orthotopic pancreatic cancer models

All animal experiments were performed in accordance with current UK legislation under an approved project licence (reference number: 403725). Mice were housed under specific pathogen-free conditions at the Biomedical Science Unit at the University of Liverpool. In the second model, orthotopic pancreatic tumors were initiated by implanting 1×10^6 primary KPC-derived cells into the pancreas of immune-competent syngeneic mice on a mixed background 129/SvJae/C57Bl/6. Since in this model tumors grow slower, tumors were established for three weeks before beginning treatment (Fig. 6). Syngeneic recipient mice were six- to eight-week-old female mice descended from mice used to generate the KPC-derived cells but lacked oncogenic *Kras*^{G12D} expression (PC mice). Mice were administered i.p with Gemcitabine (100 mg/kg), IGF blocking antibody commercially available from abcam (25 μ g/mouse) (abcam 9572) or IgG isotype control antibody, every 2 -3 days for 10-15 days before harvest. At endpoint, tumors were harvested, weighed, cryopreserved fixed in formalin, solubilized for RNA purification, or collagenase-digested for flow cytometry analysis and sorting of immune cell populations, tumor cells, and non-immune stromal cells. Only animals in which no tumors grew were removed from the study.

Tumor tissues were analyzed by immunohistochemistry for phospho-Insulin/IGFR expression, EpCAM expression, macrophage infiltration, fibroblast activation and apoptosis using the following antibodies: phospho-insulin/IGF receptor antibody (R&D), EpCAM (BD Pharmingen), CD68 antibody (DAKO), CD206 (abcam), α SMA (abcam) and cleaved caspase 3 (Cell signaling). Expression of *Igf-1* and *Igf-2* in TAMs, tumor cells and non-immune stromal cells were determined by qPCR. *In vivo* experiments were performed with n= 6 mice (Fig. 5) and n=9-12 mice (Fig. 6).

Analysis and quantification of immune cells in pancreatic tumors by flow cytometry

Single cell suspensions from murine pancreatic tumors were prepared by mechanical and enzymatic disruption in Hanks Balanced Salt Solution (HBSS) with 1 mg/mL Collagenase P (Roche). Cells suspension were centrifuged for 5 min at 1500 rpm, resuspended in HBSS and filtered through a 500 μ m polypropylene mesh (Spectrum Laboratories). Cells were

resuspended in 1 mL 0.05% Trypsin and incubated at 37°C for 5 minutes. Cells were filtered through a 70 µm cell strainer and resuspended in PBS + 1% BSA. Cells were blocked for 10 minutes on ice with FC Block (BD Pharmingen, Clone 2.4G2) and then stained with Sytox® blue viability marker (Life Technologies) and conjugated antibodies against anti-CD45-PE/Cy7 (Biolegend, clone 30-F11), anti-F4/80-APC (Biolegend, clone BM8), anti-CD206 PerCP/Cy5.5 (Biolegend, clone C068C2), Ly6C-PE (Biolegend, clone HK1.4), CD11b-APC (Biolegend, clone M1/70), Ly6G-PerCP/Cy5.5 (Biolegend, clone 1A8), CD8a-PerCP/Cy5.5 (Biolegend, clone 53-6.7), CD4-PE (Biolegend, clone GK1.5), anti-TCRγ/δ-APC (Biolegend, clone GL3), anti-Ly-6G/Ly-6C (Gr-1)-PerCP/Cy5.5 (Biolegend, clone RB6-8C5). Flow cytometry was performed on a FACSCanto II (BD Biosciences).

Statistical Methods

Statistical significance for *in vitro* assays and animal studies was assessed using unpaired two-tailed Student *t* test or one-way ANOVA coupled with Tukey's post hoc tests, and the GraphPad Prism 5 program. Human samples were analyzed using Fisher's exact test and the Matlab version 2006b program.

Institutional approvals

All studies involving human tissues were approved by the University of Liverpool and were considered exempt according to national guidelines. Human pancreas carcinoma samples were obtained from the Liverpool Tissue Bank and patients consented to use the surplus material for research purposes or purchased from US Biomax. All animal experiments were performed in accordance with current UK legislation under an approved project licence (reference number: 403725). Mice were housed under specific pathogen-free conditions at the Biomedical Science Unit at the University of Liverpool.

All studies involving blood collection were approved by the National Research Ethics (Research Integrity and Governance Ethics committee- Reference: RETH000807). All individuals provided informed consent for blood donation on approved institutional protocols.

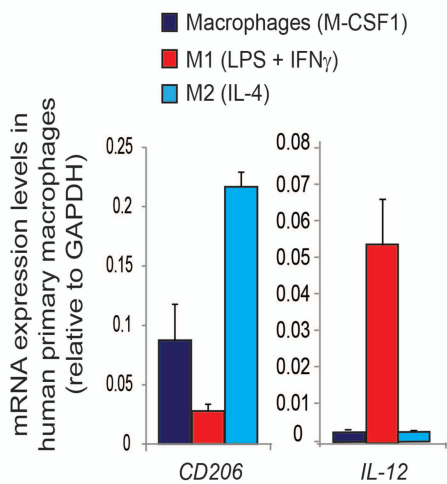
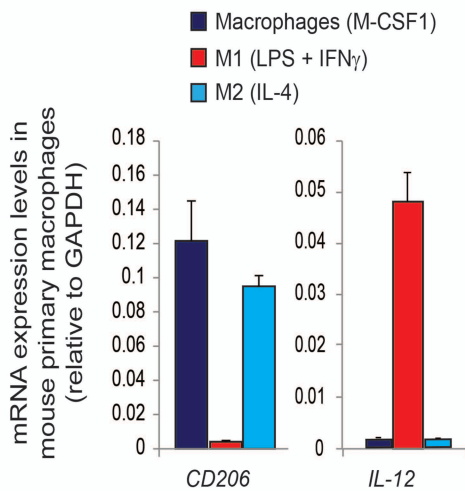
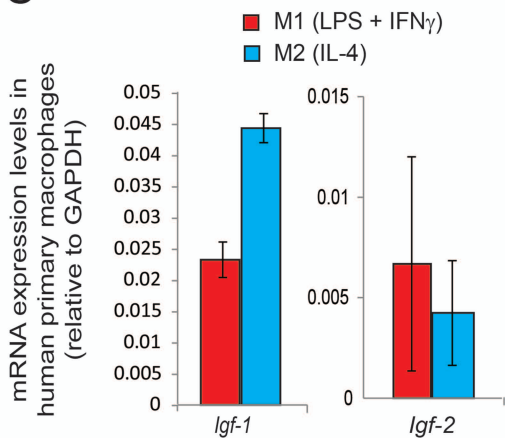
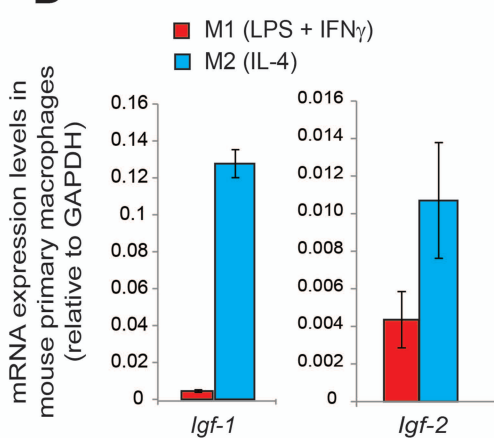
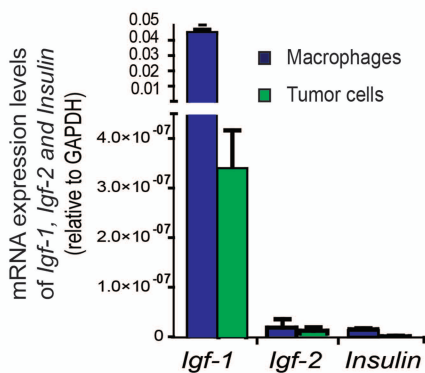
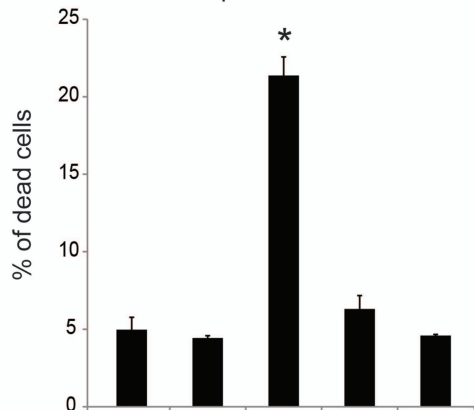
A**B****C****D****E**

Figure S1

A

Human pancreatic cancer cells



Gemcitabine:	-	-	+	-	-
MCM:	-	+	-	-	+
IGF Ab:	-	-	-	+	+

B

Primary mouse pancreatic cancer cells

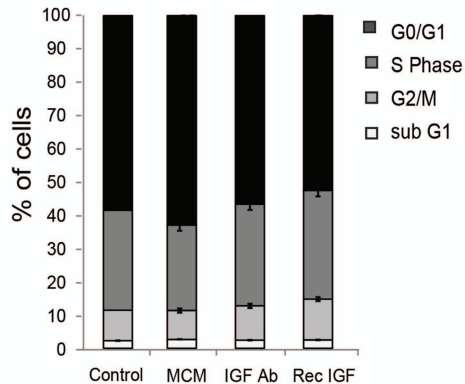
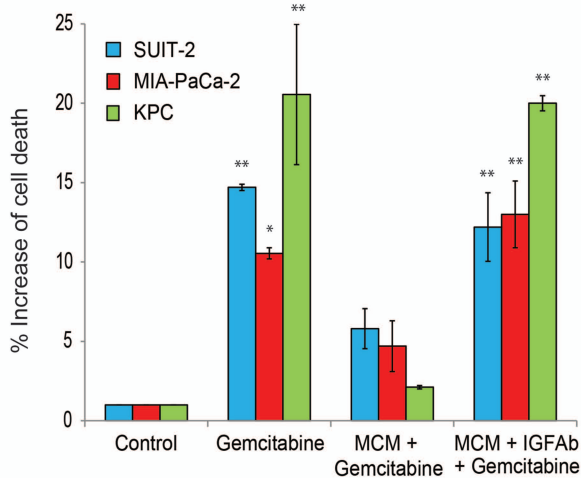
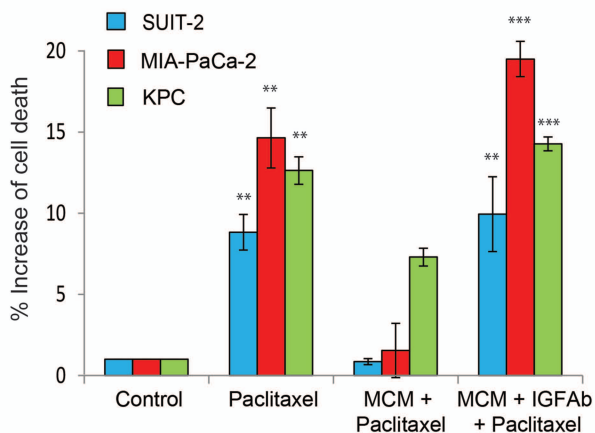


Figure S2

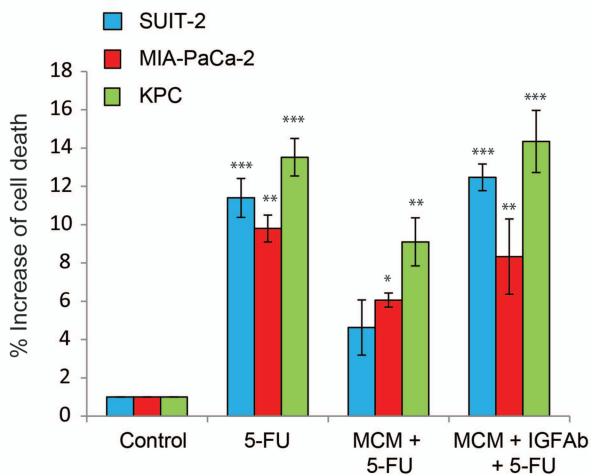
A



B



C



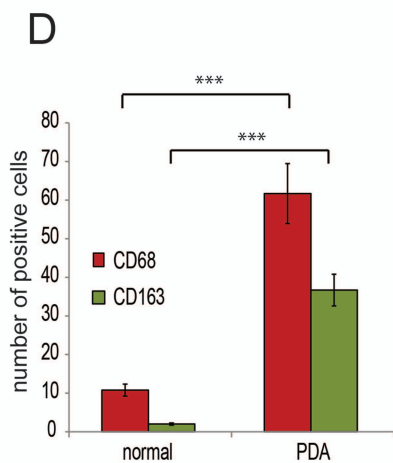
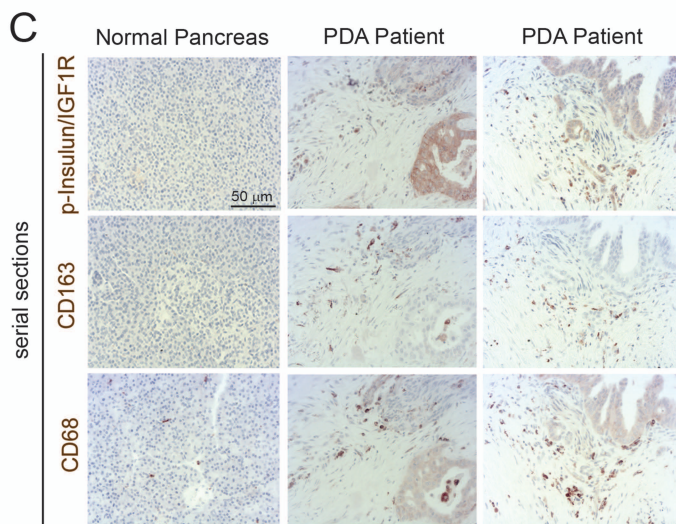
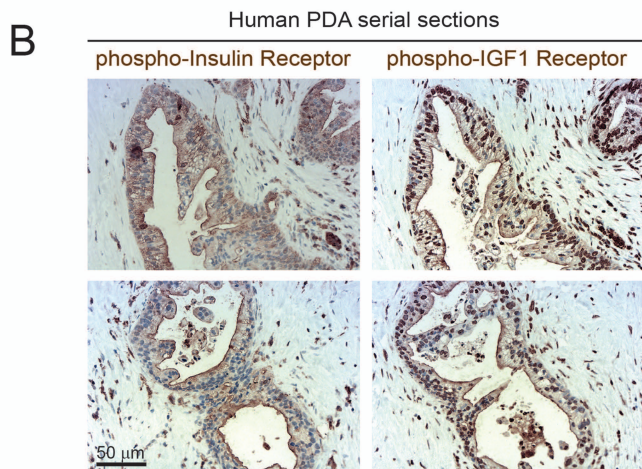
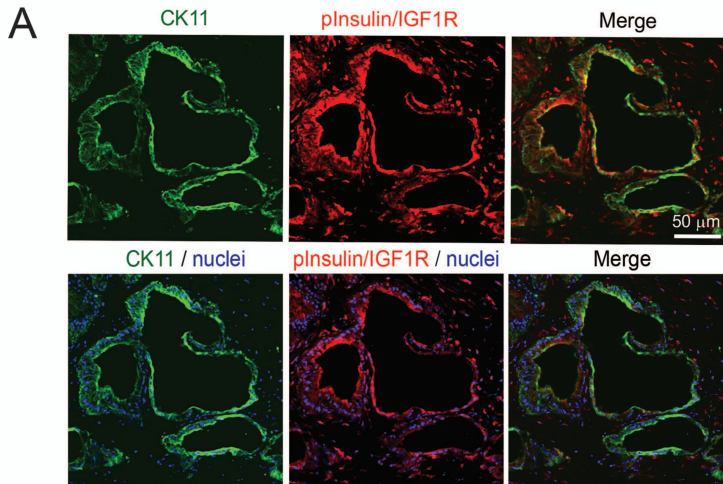


Figure S4

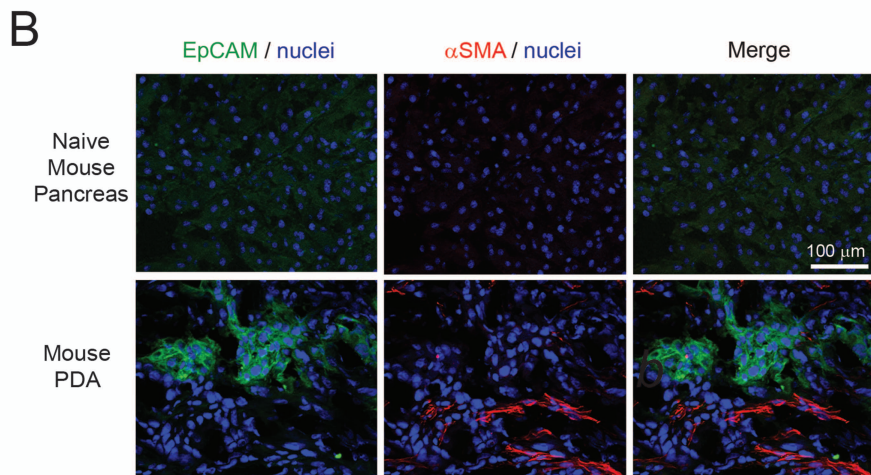
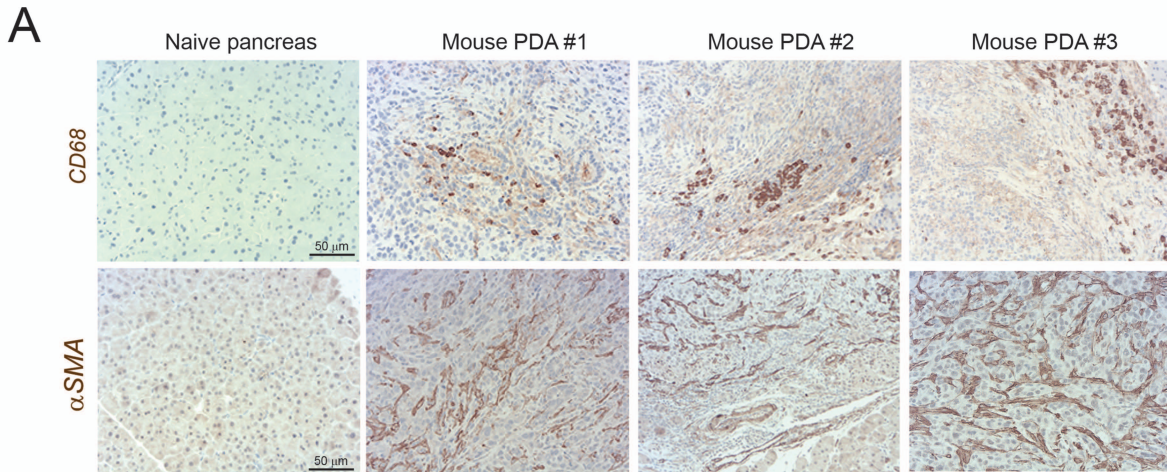
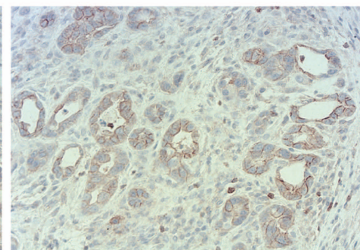
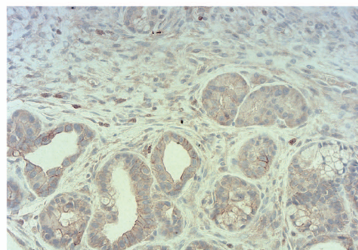
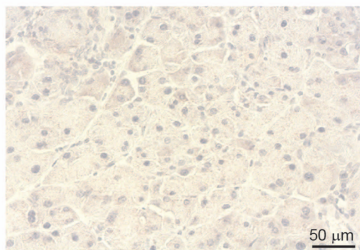


Figure S5

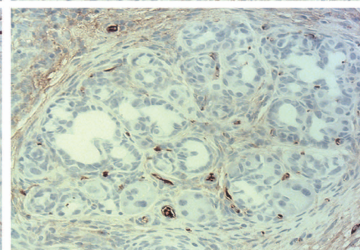
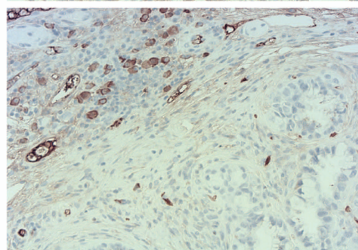
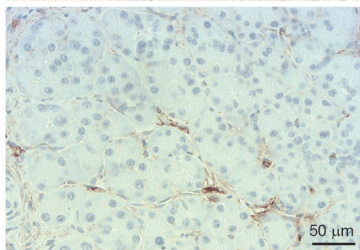
Adjacent normal pancreas

Genetically engineered KPC mouse model

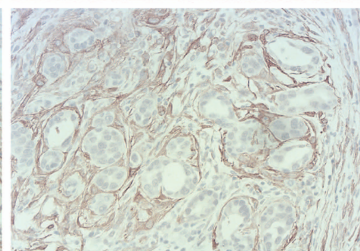
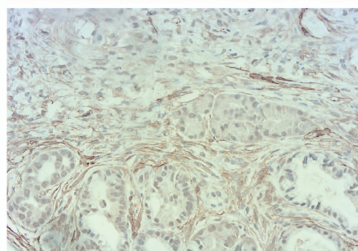
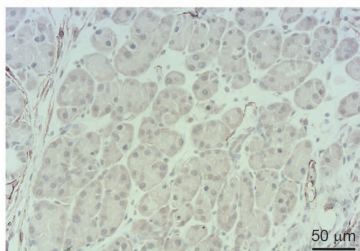
phospho-Ins/IGF1 R



CD206



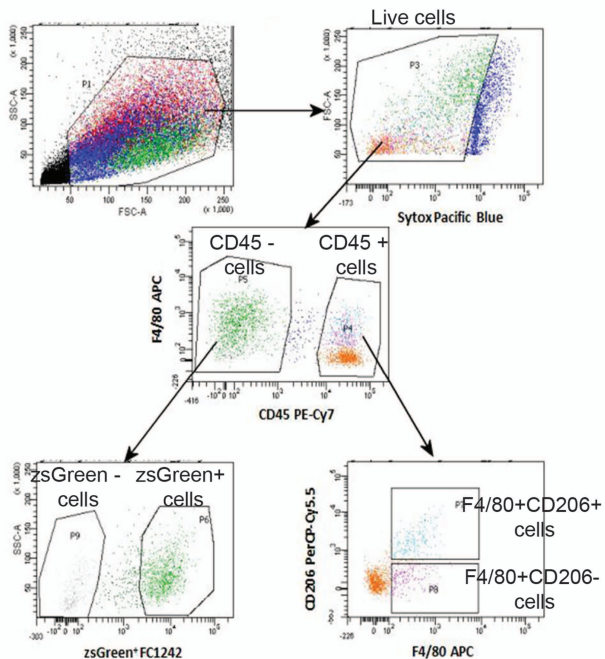
α -SMA



serial sections

Figure S6

A



B

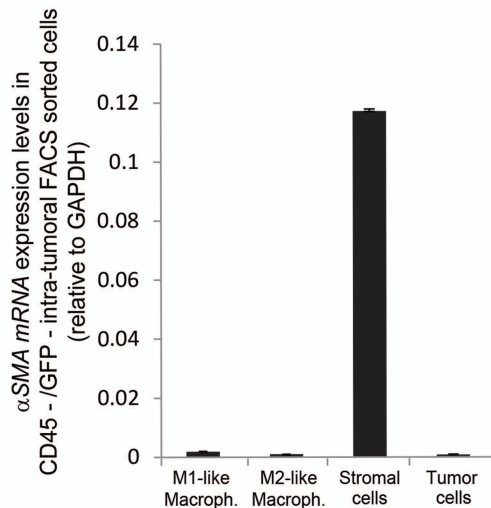


Figure S7

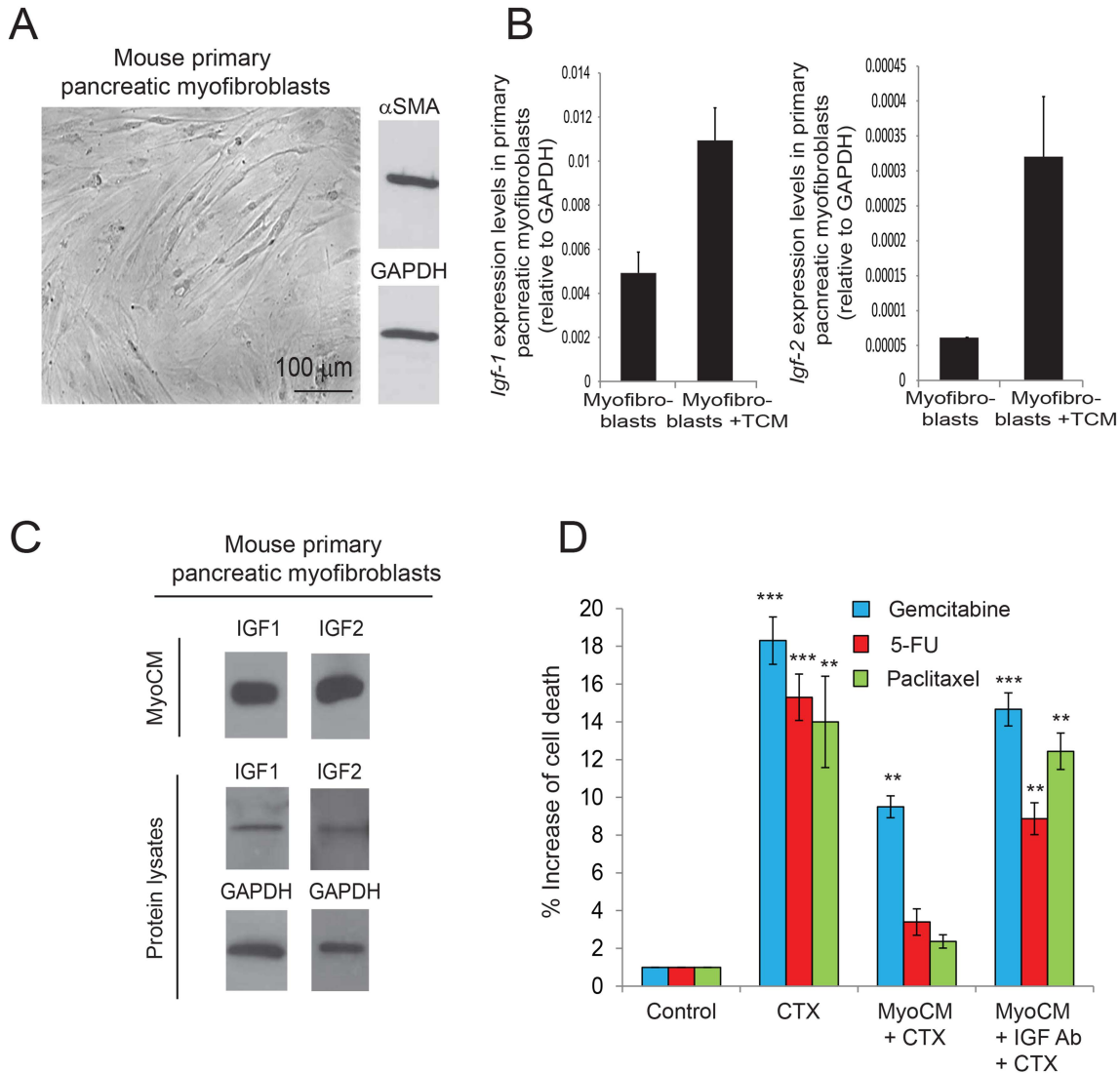
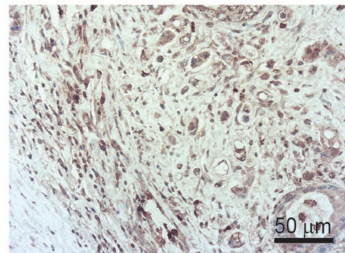
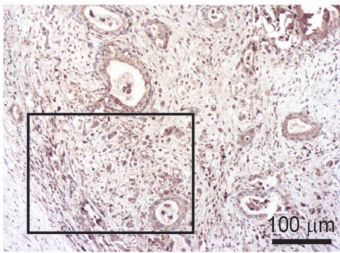


Figure S8

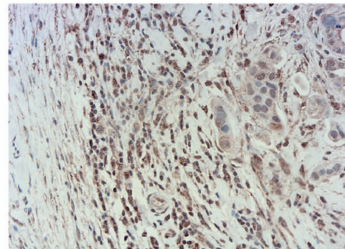
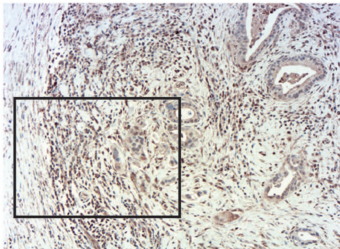
Human PDA

serial sections

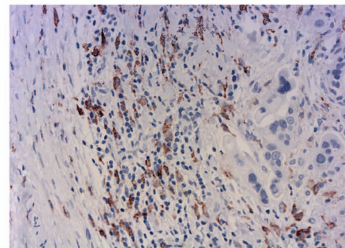
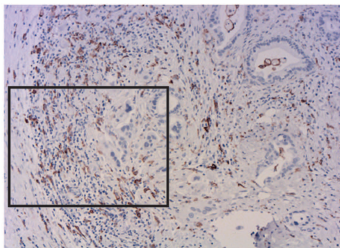
IGF-1



IGF-2



CD163



α SMA

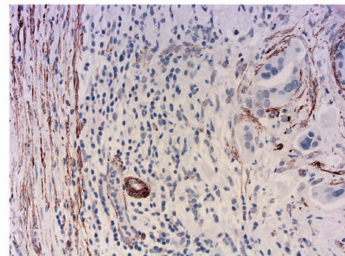
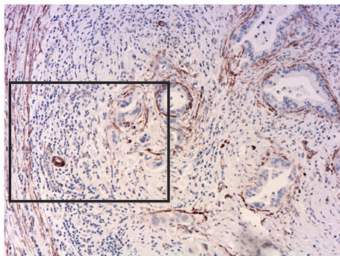
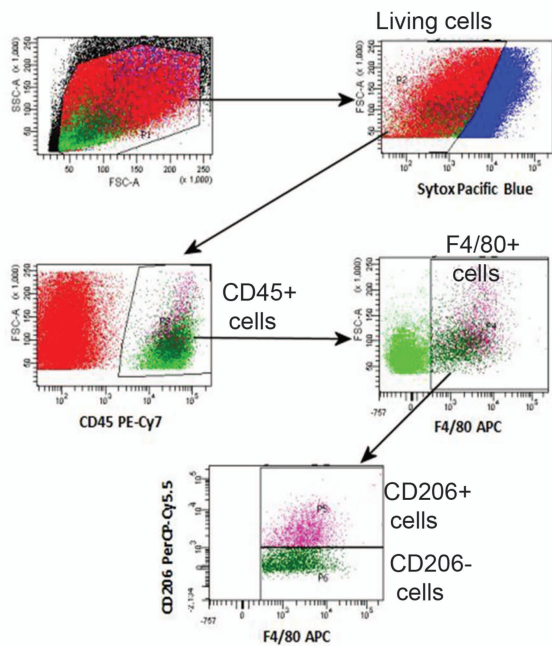
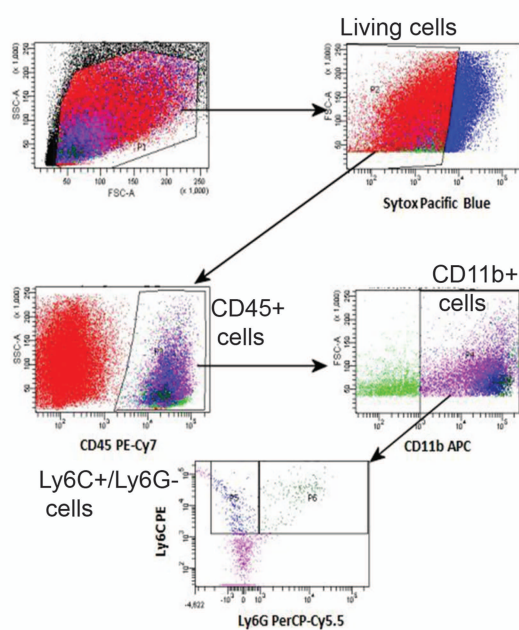


Figure S9

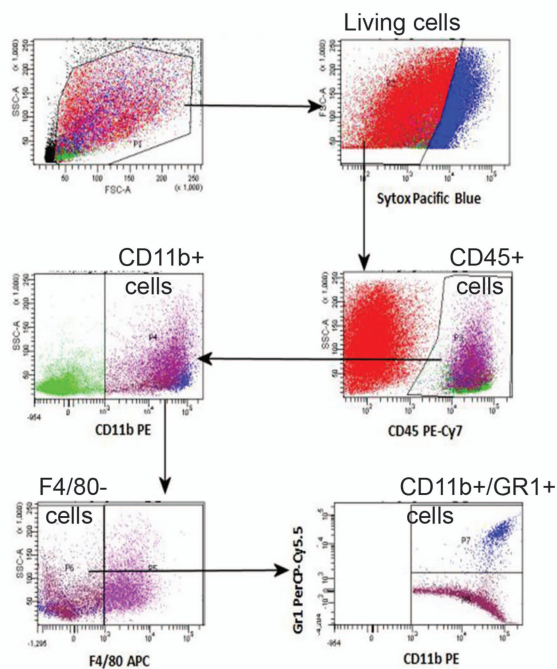
Gating strategy for macrophages



Gating strategy for inflammatory monocytes



Gating strategy for neutrophils & MDSCs



Gating strategy for T cells

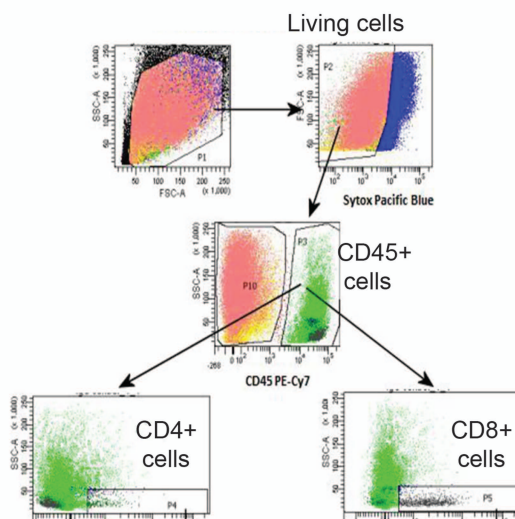


Figure S10

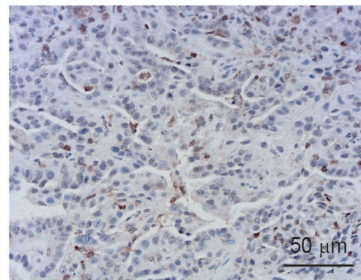
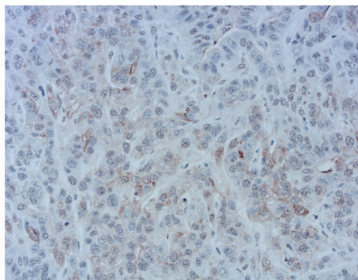
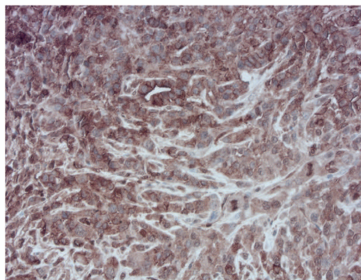
Treatment with anti-IGFs blocking antibodies

Control IgG Tx

BI 836845 Tx

ab 9572 Tx

Phospho-Insulin
Receptor



Phospho-IGF1
Receptor

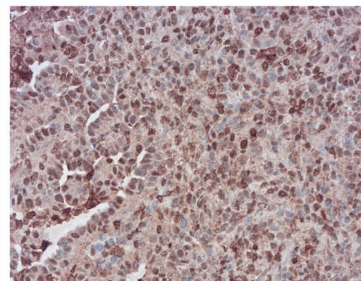
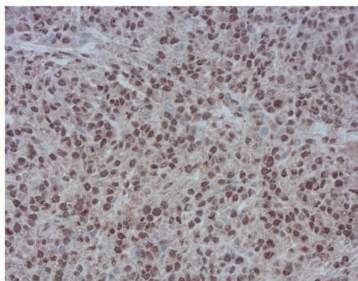
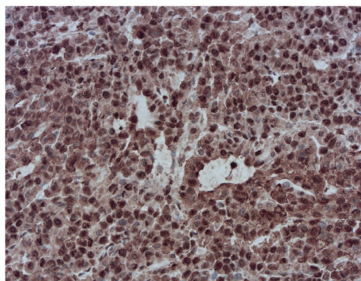
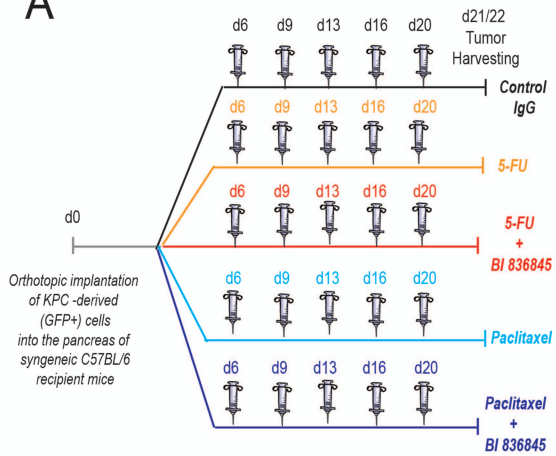
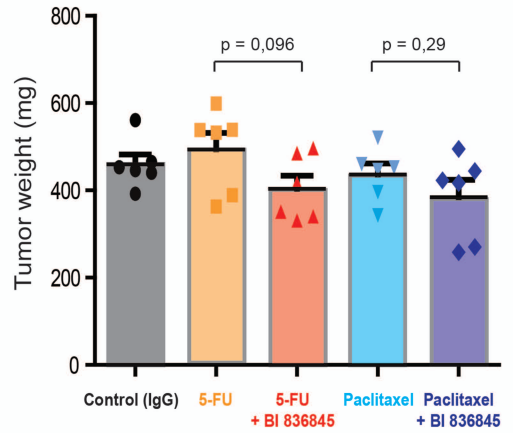
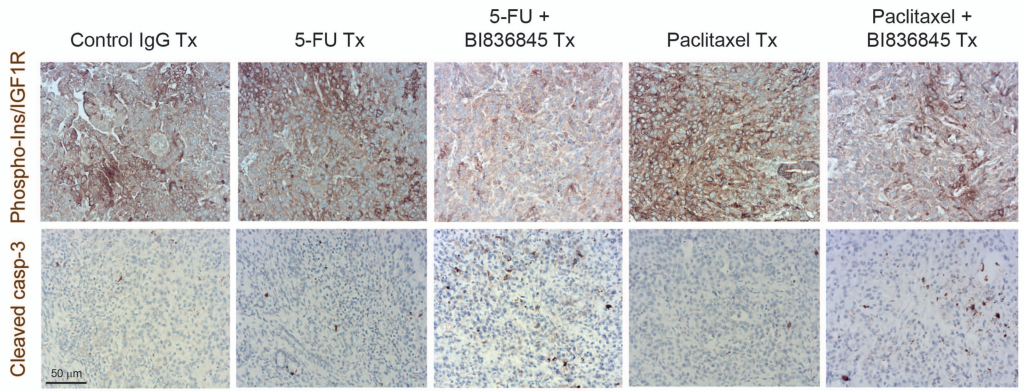


Figure S11

A**B****C****D**